ABSTRACT

Title of Dissertation: ERROR CONTROL FOR
THE MEAN CURVATURE FLOW

Omar Lakkis, Doctor of Philosophy, 2002

Dissertation directed by: Professor Ricardo H. Nochetto
Department of Mathematics

We study the equation describing the motion of a nonparametric surface according to its mean curvature flow. This is a nonuniformly parabolic equation that can be discretized in space via a finite element method. We conduct an aposteriori error analysis of the semidiscrete scheme and derive upper bounds to the error in terms of computable quantities called estimators. The reliability of the estimators is practically tested through numerical simulations.

ERROR CONTROL FOR

THE MEAN CURVATURE FLOW

by

Omar Lakkis

Dissertation submitted to the Faculty of the Graduate School of the
University of Maryland, College Park in partial fulfillment
of the requirements for the degree of
Doctor of Philosophy
2002

Advisory Committee:

Professor Ricardo H. Nochetto, Chairman/Advisor
Professor Stuart S. Antman
Professor Howard Elman
Professor Bo Li
Professor Tobias von Petersdorff
Professor Jonathan M. Rosenberg

DEDICATION

To Vera and to all the folks whose calls stayed unanswered in the last two months

ACKNOWLEDGEMENTS

The list of people whose contribution have made this dissertation possible is too long to fit on this page. I will limit myself to mention only those whose lack of contribution would have made it impossible.

Special thanks go to Kunibert "BERT" Siebert and Alfred "AL" Schmidt for introducing me to and guiding me through ALBERT (a C library for adaptive mesh refinement and finite element implementation which has been used extensively in this work).

I am indebted to Ricardo Nochetto, advisor and friend, for his help and support not only in the "scientific" aspects of this work, but also for the "material" aspects by providing adequate funds for research, for the "social" aspects for putting me in touch with high class mathematicians and last, but by no means least, for the "human" aspect — which materialized often in the "Decompressive Friday evenings at Three Brothers" in Edmonston, Maryland.

I must also thank Gerhard Dziuk, Francesca Fierro and Andreas Veeser for the insightful discussions and suggestions.

Last but not least I would like to thank Claudio Verdi for support and encouragement.

Contents

List of Figures

Chapter 1

Introduction

1.1 The mean curvature flow: a model for geometrically based motions

Geometrically based motions and their numerical approximation

Partial Differential Equations (PDE's) were conceived to model the evolution of physical phenomena on one hand, and to describe objects of differential geometry on the other hand. These two aspects can easily overlap. For example, in many cases of physical modeling, part of the phenomenon is an evolution in time of a geometric object according to some given relationship between different geometric and kinematic quantities. In this case the model is called a *Geometrically Based Motion (GBM)*.

GBM arise in various mathematical and applicative settings. The study of these highly nonlinear PDE's, both analytically and computationally, constitutes a nontrivial mathematical and numerical challenge. In recent years much effort

has been invested in order to get a better understanding of GBM and the implementation of numerical methods to simulate them. This is due not only to the interesting mathematical theories that must be developed, but also to the interest that non-mathematicians have in the solutions of such equations whose applicability fields range from Materials Science to General Relativity, from Phase Transition to Medical Imaging [HI97, MS95, SO89].

This dissertation focuses on the numerical approximation of the *mean curvature flow*, which is a model PDE describing a GBM. We investigate a finite element method that approximates the exact solution of the mean curvature flow of graphs described in section 1.2.

Aposteriori error estimates

Numerical schemes for the solution of PDE's should be implemented in both a *reliable* and an *efficient* way, so as to achieve the best accuracy possible with the least expenditure of computing time and space.

Adaptive finite element methods have provided a very useful tool for the implementation of efficient and reliable algorithms that are used in different application fields from Computational Fluid Dynamics to Materials Science.

A mathematically sound starting point for the derivation of reliable and efficient adaptive finite element methods are the *aposteriori*[1] *error estimates*. Aposteriori error estimates based adaptive methods have been used with success for linear elliptic partial differential equations starting in the late seventies [BR78].

[1]We will be using the somewhat barbaric but practical version of the Latin "a posteriori" by contracting it into "aposteriori" (See [GT83, p.3] for a similar remark). Notice that we do not italicize the Latin in the text.

These methods prove especially useful in problems which solution has localized singularities. In this case the computational effort is reduced, by reducing the amount of "wasted" resolution. The finite element meshes are adaptively designed so as to reduce this waste.

Following the pioneers there has been extensive work treating linear and, to a much less extent, nonlinear elliptic and parabolic problems during the last two decades of the past century.

The monographs by Verfürth [Ver98] and Ainsworth & Oden [AO00] survey the situation for elliptic equations. Some nonlinear situations are discussed by Verfürth, but the generality of the discussion prevents the understanding of the fine details that an ad hoc analysis might provide. This necessitates the more careful study of particular equations [FV02].

As for the parabolic problems, the most ambitious work in the literature is the series of articles by Johnson and his coworkers [EJ91]. While their coverage of the linear case is very deep and general, the one for the nonlinear case leaves much room for improvement. The ad hoc approach to these problems remains the best means to exploit successfully some particular nonlinear structure of the problem at hand, as exemplified by the articles of Nochetto, Savaré, Schmidt & Verdi [NSV00a, NSV00b].

The Mean Curvature Flow, which we will be dealing with in this dissertation, is yet another example that is not even included in the "theories" on aposteriori error estimates for nonlinear parabolic problems. A fundamental reason for this is the nonuniform parabolic nature of the equation.

Reliability of error estimators

As mentioned in the previous paragraph error estimators must satisfy two fundamental properties: reliability and efficiency. In this work we will be mainly concerned with the first aspect. We will derive upper bounds as aposteriori error estimates for the mean curvature flow of graphs. The major issue, besides establishing the mathematical results, is relating these estimates to computations by exploring how reliable the upper bounds are. In the derivation of the estimates one has to inevitably use inequalities; thus, no matter how careful is the analysis, the reliability is somewhat compromised. Hence, the estimators must be also tested practically in many different situations to obtain effective conclusions about their usefulness. The tests can be divided in two distinct categories. The first category consists of so-called *benchmark problems* of which the exact solution is known; the true error can be evaluated and compared to the estimators providing a *reliability measure* of the upper bound. The second category of tests consists of problems where the exact solution is not entirely known; here we can track the *experimental asymptotic behavior* of the estimators by successive global refinements of the mesh.

1.2 What is the Mean Curvature Flow (MCF) and what motivates its study

Let $T \in \mathbb{R}^+$ and $\Gamma(t)$ be a codimension 1 submanifold (with or without boundary) of a Riemannian manifold $\mathscr{M}$, for each $t \in [0, T]$. That is, we give ourselves a real-parameter family of submanifolds. The real parameter is thought of as *time*. Although the theory of MCF goes through in a very general setting as in

Ambrosio's notes [Amb97], in our study we will be dealing with the case of proven physical relevance in which $\mathscr{M}$ is the Euclidean space $\mathbb{R}^{d+1}$ with $d \in [1:3]$. Thus $\Gamma(t)$ is either a plane curve, or a surface in space, or a 3-submanifold of the 4-dimensional space. We refer to $\Gamma(t)$ as "surface" in all these cases, although $\Gamma(t)$ might actually not be a 2-dimensional manifold.

The family of surfaces $\{\Gamma(t)\}_{t\in[0,T]}$ is said to be a *Mean Curvature Flow (MCF)* if at each instant $t \in [0,T]$ and at each non-boundary point $\boldsymbol{x} \in \Gamma(t)$ the normal velocity vector $\boldsymbol{V}(\boldsymbol{x},t)$ $\boldsymbol{x} \in \Gamma(t)$ is negatively proportional to the mean curvature $\boldsymbol{H}(\boldsymbol{x},t)$, that is

$$\boldsymbol{V}(\boldsymbol{x},t) = -\boldsymbol{H}(\boldsymbol{x},t). \tag{1.1}$$

Let $\boldsymbol{\nu}(\boldsymbol{x},t)$ be a choice of a normal vector such that

$$\boldsymbol{H}(\boldsymbol{x},t) = -\frac{1}{d}(\kappa_1(\boldsymbol{x},t) + \cdots + \kappa_d(\boldsymbol{x},t))\boldsymbol{\nu}(\boldsymbol{x},t), \tag{1.2}$$

where the $\kappa_i(\boldsymbol{x},t)$ are the principal curvatures of $\Gamma(t)$ at $\boldsymbol{x}$ (this is the "inward" normal for a sphere). We can then introduce the *(scalar) normal velocity* $V(\boldsymbol{x},t) := \boldsymbol{V}(\boldsymbol{x},t)\cdot\boldsymbol{\nu}$. By multiplying both members of (1.1) by $\boldsymbol{\nu}$ we obtain the following scalar equation

$$V(\boldsymbol{x},t) = -\frac{1}{d}(\kappa_1(\boldsymbol{x},t) + \cdots + \kappa_d(\boldsymbol{x},t)). \tag{1.3}$$

Conversely, assuming that the flow of the family $\{\Gamma(t)\}$ is normal and that (1.3) is satisfied, then it follows that (1.1) is satisfied.

If the *initial surface* $\Gamma(0)$ is given, we pose the problem of determining the whole flow $\Gamma(t)$ as t ranges in $(0,T)$, assuming it obeys (1.1).

Mean curvature flow of graphs

If we look at a portion of $\Gamma(t)$ (named again $\Gamma(t)$) that can be represented as the graph of a function $u : \Omega \subset\subset \mathbb{R}^2 \to \mathbb{R}$, then the equation (1.3) can be written as

$$\frac{\partial_t u(x,t)}{\sqrt{1+|\nabla u(x,t)|^2}} - \frac{1}{d}\,\mathrm{div}\,\frac{\nabla u(x,t)}{\sqrt{1+|\nabla u(x,t)|^2}} = 0, \qquad \text{for } x \in \Omega, t \in [0,T] \tag{1.4}$$

where ∇ is the derivative with respect to x. This is the so called *Mean Curvature Flow of Graphs*.

The study of (1.4) is important, not only to understand the local behavior of the MCF as a geometrically based motion, but equation (1.4), with suitable boundary conditions imposed on $\partial\Omega$, arises in free boundary problems in fluid dynamics [Bän01]. Anisotropic versions of (1.4) are encountered also in phase transition problems [FV01, DD00]

Also, by adding one more spatial dimension — that is, $\Omega \in \mathbb{R}^3$ instead of $\mathbb{R}^2$ — and replacing $1+|\nabla u|^2$ with $\varepsilon^2+|\nabla u|^2$ in the denominators, it is possible to obtain the level-set formulation of the MCF and find a viscosity solution, by taking the limit for $\varepsilon \to 0$. Notice that the Level Set formulation is a powerful way of describing the MCF which handles topological type changes in the family $\Gamma(t)$ [Amb97, ES91].

Examples of Mean Curvature Flow

A basic yet important example of a surface moving by mean curvature is given by the following:

1.2.1 Example (Shrinking Sphere)**.** Let $r : [0,T) \to \mathbb{R}^+$. If $\mathbb{S}^d$ denotes the unit sphere in $\mathbb{R}^{d+1}$, we can associate to r the family of spheres

$$\left\{S(t) :\ S(t) := r(t)\mathbb{S}^2,\ t \geq 0\right\}. \tag{1.5}$$

We pose now the question of determining r such that this family is a mean curvature flow.

According to our convention the curvature vector of the sphere points outward and is a constant as a function on the sphere $S(t)$ at a given time t. This constant is given by $1/r(t)$ since $r(t)$ is the radius of the sphere. Also this implies that the normal velocity is given by $\mathrm{d}_t r(t)$. Thus equation (1.3) becomes

$$\mathrm{d}_t r(t) = -\frac{1}{r(t)}, \tag{1.6}$$

which implies

$$r(t) = \sqrt{r(0)^2 - 2t}. \tag{1.7}$$

Thus the sphere $S(t)$ is shrinking in time, and reduces to a point at time $t = r(0)^2/2$. For a thorough discussion of this example, the reader is referred to the seminal work of Huisken [Hui84], and for a discussion on "what happens after the point singularity" it is worth reading the beautiful articles of Evans & Spruck [ES91] and Chen, Giga & Goto [CGG91].

For a visualization of this phenomenon we refer to Figure 1.1. There we represent a portion of the sphere as a graph of a function. When the shrinking sphere portion becomes vertical at a boundary point of the square, the gradient blows up and it develops a singularity. (This is an singularity of analytic nature, due to the limitations of the graph formulation; it is different than, and not to be confused with, the point singularity of geometric nature described above). This singularity will be described in details in Chapter 2 and will be also used for the benchmark computations of Chapter 4.

This is shown in the sequence of snapshots in Figure 1.1, taken from a computer simulation of the MCF via a finite element code. The code is written in

C and relies on the ALBERT library [SS00]. We used GLTools to produce the graphics.

1.2.2 Example (Planar angle becoming a soap film)**.** The Mean Curvature Flow with Dirichlet prescribed boundary conditions evolves a give initial condition into a minimal surface, when the forcing term is zero. This allows to construct many examples. For instance if the initial condition is given by

$$u(x, y; 0) = |1 - x - y|$$

on the square domain $[0, 1] \times [0, 1]$, we can see a sharp angle between two planes evolving into a smooth surface which becomes closer to a minimal surface with time.

In the same spirit we can give another example that will be used also in Chapter 4.

1.2.3 Example (A cone becoming a catenoid)**.** If the MCF of graphs is taken with zero forcing term and constant boundary values on the boundary of the annulus $\Omega = \mathrm{B}_1(0) \setminus \overline{\mathrm{B}_{1/2}(0)}$. If the initial condition is a truncated cone, that has zero height at the external circle of $\partial\Omega$ and has height H at the internal circle, then the solution is a flow of a graph from the truncated cone into a catenoid as shown in Figure 1.3. The catenoid is the minimal surface spanning two coaxial circles.

Again here, the graph formulation leads to singular solution in some case. The development of singularities happens for certain values of H. If $H < H^* := \log(2 + \sqrt{3})/2$ there no singularities. If $H = H^*$ a singularity forms "at time $T = \infty$" (so technically there are no singularities), and for $H > H^*$ a singularity appears in finite time [Ura94]. This will lead to interesting numerical experiments.

As a last example in this introduction we show a curiosity which illustrates once more the smoothing feature of the MCF.

1.2.4 Example (From an egg box to a crown)**.** We take a highly oscillatory initial condition on the square and flow it with our code. The results are shown in Figure 1.4.

1.3 Plan of the dissertation

In Chapter 2 we state the initial boundary value problem that will be studied. Its basic properties of like stability estimates are established. We also show how to derive a weak form that allows a finite element discretization in space. Appendix A should be referred to whenever notation doesn't look familiar.

We the proceed to Chapter 3 which constitutes the central part of this work. Here we develop a theory of aposteriori based error estimation. We first show some basic geometric relations that are crucial for the analysis. We also introduce the concept of error, indeed Sobolev norms do not allow to derive any satisfactory estimate.

In deriving the estimates for the MCF of graphs we incidentally find ourselves discovering new estimates for the simpler case of the heat equation. This secondary result, which is unpublished, has hence been included in Section A.3. Its proof is simpler than the one for the MCF and it will be helpful to read it before reading Chapter 3.

Finally, in Chapter 4 we present results from our computer simulations efforts. The main purpose of this chapter is to show that the error bounds derived in Chapter 3 are meaningful in practical cases.

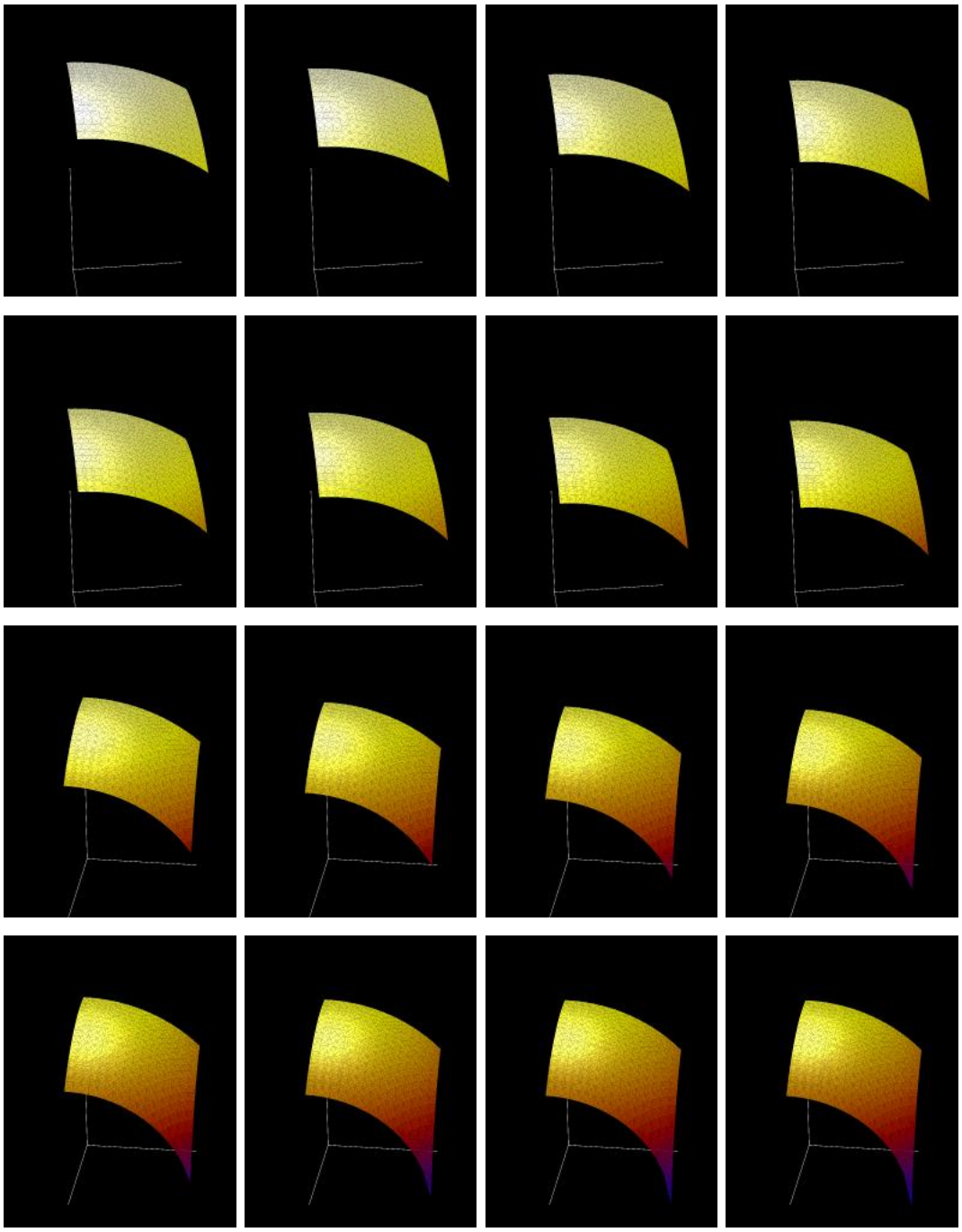

Figure 1.1: A sphere moving by mean curvature shrinks to a point in finite time. If we represent a portion of a moving sphere as a graph of a function on a square domain in the plane, we obtain a parabolic equation (the MCF for graphs) which has a solution that develops a singularity on the boundary in finite time.

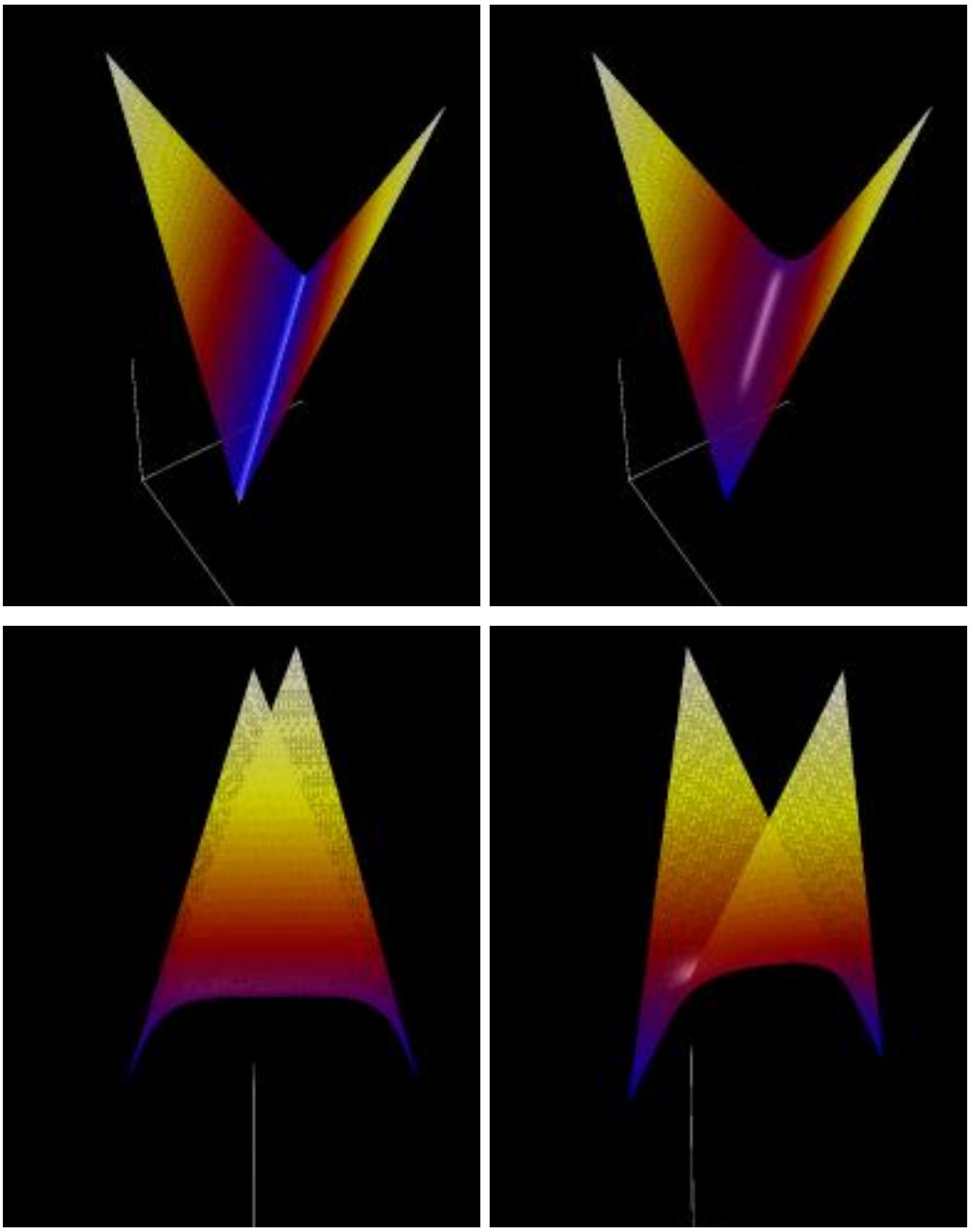

Figure 1.2: A planar angle becomes a soap film. This is a parabolic smoothing feature of the MCF. The non-smooth initial surface evolves into a minimal surface. Minimal surfaces are used in architecture to construct beautiful and amazingly stable structures like München's Olympic stadium rooftop designed by Frei Otto in the late sixties.

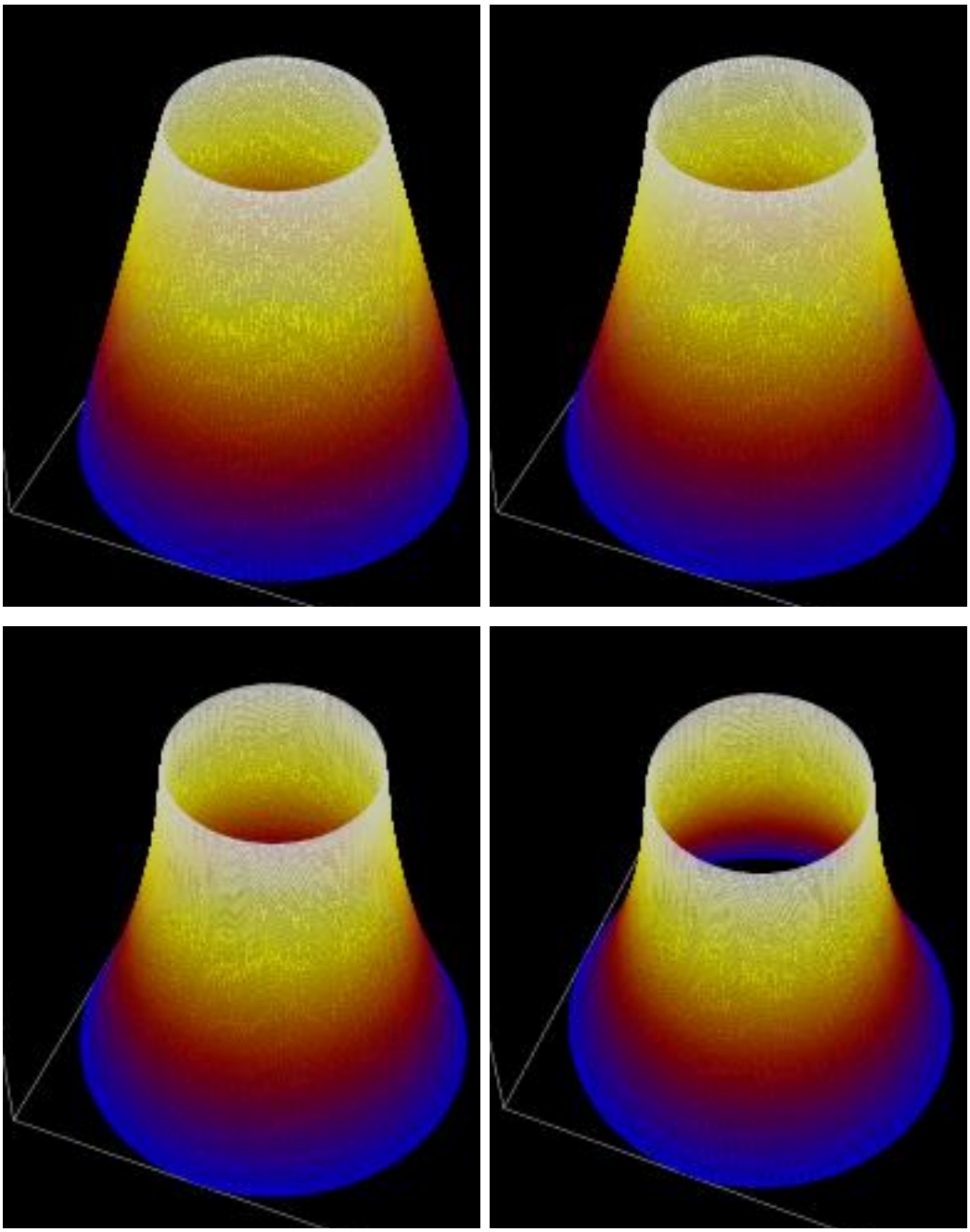

Figure 1.3: Catenoids are the only axially symmetric minimal surfaces. A solution of the MCF that starts from a cone, evolves into a catenoid when this surface is a graph of a function in the annulus. Otherwise, the solution develops a singularity in finite time.

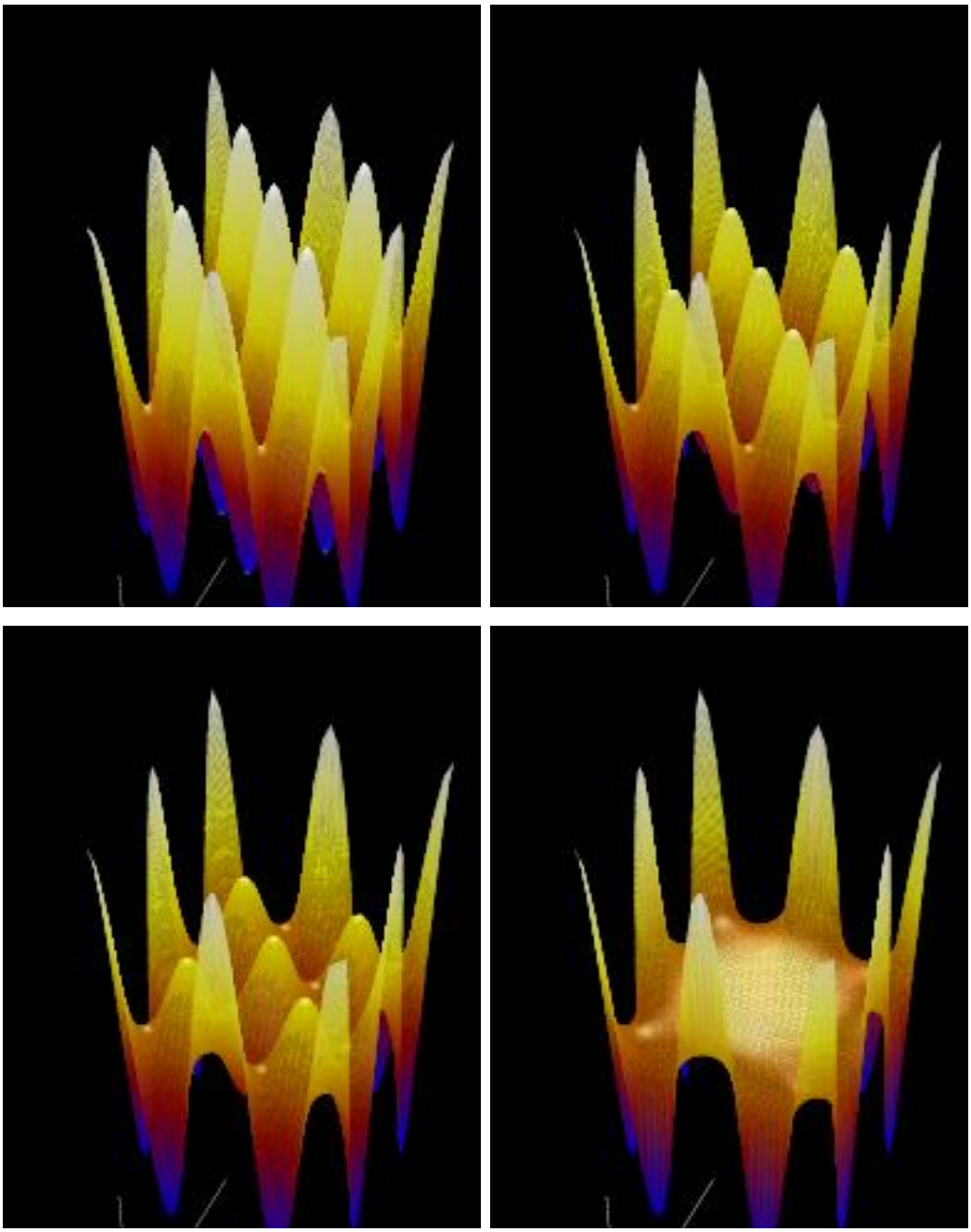

Figure 1.4: As seen by this series of snapshots the MCF has a very nice smoothing property, due to the parabolic nature of the equation. The behavior is somewhat similar to that of the heat equation, as long as gradients are small.

Chapter 2

The Mean Curvature Flow of Graphs and its Approximation via Semidiscrete Finite Element Approximation

In this chapter we introduce precisely the initial-boundary value problems that will be studied. We then review very briefly some partial differential equation theory related to these problems and provide our blanket assumptions on solvability and regularity. The weak form is then introduced and some useful stability results are established. Finally we introduce the space-discretization of the equations via a finite element method.

2.1 The Cauchy-Dirichlet problem for the MCF of graphs

Let us start by introducing some definitions and *hypotheses that will be assumed throughout the dissertation*. Should we ever need to relax or strengthen them, we will explicitly state it.

Most of the basic notation used here and in the subsequent chapters is defined in appendix A.

2.1.1 Hypothesis (Domain regularity)**.** *Let $d \in \{2, 3\}$ we denote by $\Omega \subset \mathbb{R}^d$ a connected and bounded set whose boundary $\partial\Omega$ is a finite union of Lipschitz $(d-1)$-dimensional sets. The set Ω is also assumed to lie on one side of its boundary.*[1] *(For details, see the definition in Evans & Gariepy's book [EG92, Section 4.2, p. 127].)*

2.1.2 Definition (Elementary surface area, surface normal and normal velocity of graphs)**.** We will use extensively restrictions of the following nonlinear operators

$$\begin{aligned} Q : \mathrm{W}^1(\Omega) \ni w \mapsto & Q[w] := (1 + |\nabla w|^2)^{1/2} \in \mathrm{L}_1^{\mathrm{loc}}(\Omega); \\ N : \mathrm{W}^1(\Omega) \ni w \mapsto & N[w] := (\nabla w; -1)/Q[w] \in \mathrm{L}_\infty(\Omega)^d; \\ V : \mathrm{W}^1(\Omega \times (0,T)) \ni w \mapsto & V[w] := \partial_t w/Q[w] \in \mathrm{L}_1^{\mathrm{loc}}(\Omega \times (0,T)). \end{aligned}$$

For each function w in the spaces above $Q[w](x)$, $N[w](x)$ and $V[w](x,t)$ are respectively the *elementary surface area*, the *normal vector* and the *normal velocity* of graph w at the point $(x, w(x))$ (or $(x, w(x,t)$ if w depends on time).

Since the use of these operators is very frequent we will drop the square brackets and write Qw, Nw, Vw for short whenever this is not a source of confusion. The restrictions of these operators to subspaces of their domain will be indicated by the same symbols.

---

[1] We will refer to this kind of domain as a *Lipschitz domain*, and accordingly we will talk about C^k *domains*. Notice that it's crucial that the domain lie on one side of the boundary. Assuming smoothness of the boundary alone is not enough.

2.1.3 Problem (Cauchy-Dirichlet problem for the MCF)**.** *Given two functions* $f : \Omega \times (0,T] \to \mathbb{R}$*, and* $g : \partial_{\mathrm{p}}(\Omega \times (0,T)) \to \mathbb{R}$*; find* $u : \overline{\Omega} \times [0,T] \to \mathbb{R}$ *such that*

$$\frac{\partial_t u(x,t)}{Qu(x,t)} - \operatorname{div} \frac{\nabla u(x,t)}{Qu(x,t)} = f(x,t), \text{ for } (x,t) \in \Omega \times (0,T]; \tag{2.1}$$

$$u(x,t) = g(x,t), \text{ for } (x,t) \in \partial_{\mathrm{p}}(\Omega \times (0,T)). \tag{2.2}$$

2.1.4 Remark (Accelerated MCF)**.** Notice that the factor $1/d$ in front of the divergence in the mean curvature flow equation has been dropped (and will be dropped consistently from now on). The reason for this is to keep with the custom in related work in the literature. Thus we are actually dealing with an "accelerated" mean curvature flow: i.e., $u : \Omega \times [0,T] \to \mathbb{R}$ is a solution of (2.1) with $f = 0$ if and only if $u^{\#} : \Omega \times [0,dT] \to \mathbb{R}$, where $u(x,t) = u^{\#}(x,dt)$, is a solution of the original equation (1.4). It is important to keep this in mind when relating to examples from geometry.

2.2 Solvability and regularity

In this section we address fundamental questions regarding Problem 2.1.3 mainly by quoting known result and providing assumptions, some of which will hold throughout the dissertation. We will deal with classical solutions, but will allow singular boundary gradient behavior.

Uniqueness of a solution $u \in \mathrm{C}^{2,1}(\Omega \times (0,T])$ for 2.1.3 follows from the basic maximum principle for quasilinear parabolic equations in Lieberman's book [Lie96, Theorem 9.3].

As for existence, the most noteworthy result in the literature is given by

2.2.1 Theorem (Solution of the Cauchy-Dirichlet problem)**.** *[Lie96, 12.8] Let Ω be a C^2 domain and let γ denote the mean curvature of $\partial\Omega$ (a function defined thereon). If $g \in \mathrm{C}^{1+\alpha}(\partial_{\mathrm{p}}(\Omega \times (0,T]))$ and*

$$|f(x,t)| \leq (d-1)\gamma(x), \quad \forall x \in \partial\Omega, t \in (0,T], \tag{2.3}$$

then there exists a unique solution u in $\mathrm{C}^{2,1}(\Omega\times(0,T])\cap\mathrm{C}^0(\overline{\Omega}\times[0,T])$ to Problem 2.1.3.

Since we will be considering more general situations, ones where the sufficient conditions for existence are not satisfied, we have to assume that a solution exists (uniqueness still follows from maximum principle). For example, we will consider the Cauchy-Dirichlet problem on polygonal and non-convex domains which are not covered by Theorem 2.2.1. Notice that the subtle relationship between the mean curvature of the boundary $\partial\Omega$ and the right-hand side term f given by (2.3) Consequently we always assume the

2.2.2 Hypothesis (Classical solvability)**.** *Problem 2.1.3 admits a classical solution u in $\mathrm{C}^{2,1}(\Omega \times (0,T]) \cap \mathrm{C}^0(\overline{\Omega} \times [0,T])$.*

2.2.3 Remark (Data regularity)**.** It is worth emphasizing two rather obvious consequences of Hypothesis 2.2.2; namely

$$f \in \mathrm{C}^0(\Omega \times (0,T)) \tag{2.4}$$

$$g \in \mathrm{C}^0(\partial_{\mathrm{p}}(\Omega \times (0,T))). \tag{2.5}$$

As for the contact angle we always require

2.2.4 Hypothesis (Boundary regularity of contact angle)**.** *If u solves 2.1.3 it satisfies*

$$\frac{\nabla u}{Qu} \in \mathrm{W}^1_d(\Omega). \tag{2.6}$$

for all $t \in [0,T]$.

2.2.5 Hypothesis (Regularity of normal velocity)**.** *If* u *is the solution of 2.1.3 then it satisfies*

$$\frac{\partial_t u}{Qu} \in \mathrm{L}_d(\Omega), \tag{2.7}$$

for all $t \in [0,T]$.

2.2.6 Remark (Discussion of Hypothesis 2.2.4)**.** Property (2.6) is needed in order to apply Gauss-Green formula A.2.2 to equation (2.1), the solution u being considered to be merely continuous up to the boundary in 2.2.2. This will allow us to introduce the weak form in Section 2.3.

Notice that requiring (2.6) is not so demanding as $\nabla u \in \mathrm{C}^0(\overline{\Omega})$, in fact $\nabla u/Qu$ is automatically in $\mathrm{L}_\infty(\Omega)$. This allows to apply the Gauss-Green formula with less requirements from the ∇u at the boundary, than in the case of the heat equation for example.

It is also worth noticing that while

$$\partial^2 u \in \mathrm{L}_2(\Omega) \tag{2.8}$$

is sufficient for (2.6) to hold, in dimension $d = 2$, it is far from being necessary. This allows us to include in the discussion mild blow-up situations in which the gradient of the solution becomes infinite at the boundary, as illustrated by the following example.

2.2.7 Example (Shrinking sphere portion)**.** We look at the shrinking sphere of Example 1.2.1 from a graph perspective. To do this, let us assume that the initial radius of the sphere $r(0)$ equals 2, that its center is located at $(0,0,0)$ and that we are looking at the portion of the surface that lies above $[0,1]\times[0,1]\times\{0\}$.

In view of remark 2.1.4 and relation (1.7), this surface is given by the graph of the function

$$u : [0,1] \times [0,1] \times [0,T] \to \mathbb{R}$$
$$(x^1, x^2; t) \mapsto \sqrt{r(0)^2 - 4t - |x^1|^2 - |x^2|^2}.$$

It follows that a blow-up in the gradient occurs at point $(1, 1; 1/2)$. The solution at time $t = 1/2$ is thus singular. Indeed, the gradient

$$\nabla u(1/2) = -\operatorname{id}/u(1/2) \notin \mathrm{L}_2([0,1]^2) \tag{2.9}$$

and the second derivatives

$$\partial_{i,j} u(x^1, x^2; 1/2) = -\frac{\delta_{i,j}}{u(1/2)} - \frac{x^i x^j}{u(1/2)^3}, \tag{2.10}$$

implying $\partial^2 u(1/2) \notin \mathrm{L}_2([0,1]^2)$, whereas

$$\frac{\nabla u(1/2)}{Qu(1/2)} = \operatorname{id} \in \mathrm{W}_2^1(\Omega). \tag{2.11}$$

That is, (2.6) is satisfied but not (2.8).

Sometimes we will also need the

2.2.8 Hypothesis (Boundary regularity of time derivative)**.** *The solution u of 2.1.3 satisfies*

$$\partial_t u(t) \in \mathrm{W}_2^1(\Omega), \quad \forall t \in [0,T]. \tag{2.12}$$

This hypothesis be needed in deriving the stability estimates in Lemma 2.4.1.

2.3 Weak form of the MCF of graphs

2.3.1 Proposition (Weak form of the Cauchy-Dirichlet problem)**.** *Let $u \in \mathrm{C}^{2,1}(\Omega \times (0,T]) \cap \mathrm{C}^0(\overline{\Omega} \times [0,T])$ be a given function that satisfies Hypotheses*

2.2.4 and 2.2.5. The function u is a solution of Problem 2.1.3 if and only if

$$\int_\Omega \frac{\partial_t u(t)}{Qu(t)}\phi + \frac{\nabla u(t)\cdot\nabla\phi}{Qu(t)} = \int_\Omega f(t)\phi, \quad \forall\phi\in\mathring{\mathrm{W}}{}^1_1(\Omega), t\in[0,T]; \tag{2.13}$$

$$u(t)-\tilde{g}(t)\in\mathring{\mathrm{W}}{}^1_1, \quad \forall t\in(0,T); \tag{2.14}$$

$$u(0)=g(0) \tag{2.15}$$

where $\tilde{g}(t)$ is an extension[2] *of $g(t)$.*

Proof Suppose that u solves 2.1.3 and satisfies (2.6) and (2.7), then if $\phi\in\mathring{\mathrm{W}}{}^1_1$ then we can multiply it with both members of (2.1) and integrate in space over Ω to obtain

$$\int_\Omega f(t)\phi = \int_\Omega \left(\frac{\partial_t u(t)}{Qu(t)} - \operatorname{div}\frac{\nabla u(t)}{Qu(t)}\right)\phi \tag{2.16}$$

$$= \int_\Omega \frac{\partial_t u(t)}{Qu(t)}\phi + \int_\Omega \frac{\nabla u(t)}{Qu(t)}\nabla\phi, \tag{2.17}$$

where the second step we make used Gauss-Green formula and the fact that the trace of ϕ vanishes on $\partial\Omega$. This is legal since the proof of Theorem A.2.2 can be adapted very easily to the case $\boldsymbol{w}=\nabla u/Qu\in\mathrm{W}^1_d(\Omega)\cap\mathrm{L}_\infty$ and $z=\phi\in\mathring{\mathrm{W}}{}^1_1(\Omega)$. Equation (2.14) is just a rewriting of (2.2) given the fact that both $u(t)$ and $\tilde{g}(t)$ belong to W^1_2. Finally (2.14) follows also from (2.2) for $t=0$.

Conversely let u satisfy (2.6) and (2.7). If (2.13) is valid for any ϕ, by the Gauss-Green formula we have

$$\int_\Omega \left(\frac{\partial_t u(t)}{Qu(t)} - \operatorname{div}\frac{\nabla u(t)}{Qu(t)} - f(t)\right)\phi = 0, \forall\phi\in\mathring{\mathrm{W}}{}^1_1. \tag{2.18}$$

[2]The existence of such extension is guaranteed by a generalization to $p=1$ of [Neč67, Theorem 2.5.7], mentioned in [SZ90, (5.5)], as soon as $g(t)\in\mathrm{L}_1(\Omega)$. Recall that, in view of 2.2.3, $g(t)$ is continuous, which means that the extension can be taken to be more regular than W^1_1.

This implies that

$$\frac{\partial_t u(x,t)}{Qu(x,t)} - \operatorname{div} \frac{\nabla u(x,t)}{Qu(x,t)} - f(x,t) = 0, \text{for a.a. } x \in \Omega. \tag{2.19}$$

Since it is assumed that $u \in \mathrm{C}^{2,1}(\Omega \times (0,T])$, this equation must be verified for all $x \in \Omega$, which is (2.1). As for (2.1), that is an immediate consequence of $u \in \mathrm{C}^0(\overline{\Omega})$, (2.14) and (2.15). □

2.3.2 Remark (Weak form vs. weak formulation)**.** The weak form of the Cauchy-Dirichlet problem given in Proposition (2.3.1) is equivalent to the classical form, that is Problem 2.1, under suitable regularity assumptions. These assumptions, can of course be relaxed, in an attempt to develop a theory of *weak solutions* for the MCF of graphs. To the best of our knowledge at the time of writing this dissertation there is no satisfactory theory of weak solutions for Problem 2.1.3, in spite of the fact that the theory for weak solutions of non-parametric minimal surfaces can be considered complete [Giu84]. For even more general formulations of the mean curvature flow there are concepts of weak solutions like the measure theoretic one of Brakke [Bra78] and the level set approach [ES91, CGG91, Son93]. However none of these fits the equation for the mean curvature flow of graphs that we are studying.

Since we will not be dealing with weak solutions, we assume 2.2.2, that is, the *existence of classical solutions* throughout the dissertation. Notice that classical solutions can still have unbounded gradient at the boundary.

2.4 Stability estimate

In this section we provide some basic stability estimates for the solution of Problem 2.1.3.

We start with the following

2.4.1 Lemma (Stability estimate)**.** *Suppose u solves* (2.1) *and it satisfies Hypothesis 2.2.8 (in addition to the blanket assumptions). If f is bounded in Ω and $g \in \mathrm{W}_1^1(\partial_{\mathrm{p}}(\Omega \times (0,T)))$ then the following stability estimate holds*

$$\begin{aligned} &\frac{1}{2}\int_0^t \int_\Omega |Vu|^2 \, Qu + \int_\Omega Qu(t) \\ &\qquad \leq \mathrm{e}^{\int_0^t \|f\|^2_{\mathrm{L}_\infty(\Omega)}/2} \left(\int_\Omega Qg(0) + \|\partial_t g\|_{\mathrm{L}_1(\partial\Omega\times(0,t))} \right) \end{aligned} \tag{2.20}$$

Proof Multiply both sides of the equation (2.1) by the function $\partial_t u$ and integrate over the domain Ω (this is very similar to the proof of Proposition 2.3.1 but with non-homogeneous boundary data):

$$\begin{aligned} 0 &= \int_\Omega \frac{\partial_t u}{Qu} \partial_t u - \int_\Omega \operatorname{div} \frac{\nabla u}{Qu} \partial_t u - \int_\Omega f \partial_t u \\ &= \int_\Omega |Vu|^2 \, Qu + \int_\Omega \frac{\nabla u}{Qu} \cdot \nabla \partial_t u - \int_{\partial\Omega} \frac{\nabla u}{Qu} \cdot \boldsymbol{\nu} \partial_t u - \int_\Omega f \partial_t u. \end{aligned}$$

The use of the Gauss-Green formula is legitimated by the fact that u satisfies (2.6) and (2.12). Notice also that (2.7) implies that the first term is well defined.

The last two terms can be taken to the first member and bounded as following:

$$\begin{aligned} \int_{\partial\Omega} \frac{\nabla u}{Qu} \cdot \boldsymbol{\nu} \partial_t u &= \int_{\partial\Omega} \frac{\nabla u}{Qu} \cdot \boldsymbol{\nu} \partial_t g \\ &\leq \|\partial_t g\|_{\mathrm{L}_1(\partial\Omega)}; \end{aligned}$$

and

$$\begin{aligned} \int_\Omega f \partial_t u &= \int_\Omega f \sqrt{Qu} \frac{\partial_t u}{\sqrt{Qu}} \\ &\leq \frac{1}{2} \int_\Omega |Vu|^2 \, Qu + \frac{1}{2} \|f\|^2_{\mathrm{L}_\infty(\Omega)} \int_\Omega Qu. \end{aligned}$$

Since

$$\partial_t Qu(x,t) = \partial_t \sqrt{1 + |\nabla u|^2} = \frac{\nabla u \cdot \partial_t \nabla u}{Qu} \tag{2.21}$$

it follows that

$$\frac{1}{2}\int_\Omega |Vu|^2\, Qu + \mathrm{d}_t \int_\Omega Qu \leq \|\partial_t g\|_{\mathrm{L}_1(\partial\Omega)} + \frac{1}{2}\|f\|^2_{\mathrm{L}_\infty(\Omega)} \int_\Omega Qu. \tag{2.22}$$

To conclude, integrate in time on $[0,t]$ and then apply Gronwall inequality (Lemma A.2.1). □

2.4.2 Remark (Geometric interpretation of Lemma 2.4.1)**.** An interpretation of 2.20 in terms of area of the graph Γ can be given. Indeed, the second term on the left-hand side $\int_\Omega Qu(t)$ is the area of graph $u(t)$. The gives a control on the growth of the area in time in terms of data. For instance if the forcing term $f = 0$ and the boundary conditions are stationary in time, the equation implies a decrease in area until a stationary situation is reached. This happens for example when the solution converges to a nonparametric minimal surface.

2.5 A space-discrete finite element method for the MCF

In this section we finally introduce the *finite element spatial discretization* of Problem 2.1.3 based on the weak form derived in Section 2.3.

Notation

Let us start by introducing the basic tools for the finite element method.

Let $\mathscr{T}_h$ be a shape-regular triangulation (a simplicial partition) of the domain Ω. By this we mean that $\mathscr{T}_h$ is a set of simplexes $K \subset \Omega$ such that:

1. each K is a non-empty open simplex;

2. for each $K, L \in \mathscr{T}_h$, $\overline{K} \cap \overline{L}$ is a complete subsimplex of $\overline{K}$ and $\overline{L}$, that is, a subset which is either empty, a vertex, a whole edge or, for $d = 3$, a whole face;

3. for each $K \in \mathscr{T}_h$, if we define

$$\rho_K := \sup \left\{ \rho \in \mathbb{R}^+ : \ \mathrm{B}_\rho(x) \subset K \right\},$$

then $\rho_K / \operatorname{diam}(K) \geq \sigma$; where $\sigma \in \mathbb{R}^+$ doesn't depend on $\mathscr{T}_h$ (that is, σ is independent of h). We will refer to σ as the *shape (or geometric) regularity* of the triangulation

4. The union of the closures of the simplexes, $\bigcup_{K \in \mathscr{T}_h} \overline{K} =: \Omega_h$, equals Ω.

The symbol h stands for the *meshsize function* of $\mathscr{T}_h$, which is defined by[3]

$$h(x) := \begin{cases} \operatorname{diam}(K), \text{ if } x \text{ is a point of the simplex } K \in \mathscr{T}_h; \\ \operatorname{diam}(S), \text{ if } x \text{ is lying on some face } S \subset \partial K \text{ of a simplex } K. \end{cases}$$

Very often h denotes also $\|h\|_{\mathrm{L}_\infty(\Omega_h)}$; that is the *meshsize*. For any function ψ (including $\psi = h$) defined on Ω_h we denote by ψ_K its restriction to K, where $K \in \mathscr{T}_h$.

2.5.1 Remark (Domain approximation)**.** Notice that the *approximate domain* Ω_h, defined as the interior of the union of all closed simplexes $\overline{K} \in \mathscr{T}_h$, is assumed to be equal Ω, which means that the *domain is polygonal*. This is a simplifying assumption that could be removed at the cost of seriously complicating the analysis. This complication would boil down to adding an extra term in the estimates, due to the discrepancy between Ω_h and Ω. As long as the domain Ω is not wildly behaved, the assumption $\Omega_h = \Omega$ doesn't compromise our analysis.

[3]The subindex h which appears in $\mathscr{T}_h$ (and all related spaces, functions and quantities) is inconsistent, but we keep it here for historical reasons. Anytime h appears as a subscript to a function, it "means" membership to the discrete space.

2.5.2 Definition (Finite element spaces)**.** We introduce the *finite element spaces* that we will be using throughout the dissertation:

$$\mathbb{V}_h^\ell := \left\{\phi : \Omega \to \mathbb{R} :\ \phi_K \in \mathbb{P}^\ell,\ \phi \in \mathrm{W}_1^1(\Omega)\right\} \tag{2.23}$$

$$\mathring{\mathbb{V}}_h^\ell := \mathbb{V}_h^\ell \cap \mathring{\mathrm{W}}_1^1(\Omega), \tag{2.24}$$

where $\ell \in \mathbb{Z}^+$ and $\mathbb{P}^\ell$ is the space of polynomials of degree at most ℓ (in d variables). By a well known result [Cia78, Theorem 2.2.3] these spaces are seen to consist of continuous functions (thus using W_2^1 instead of W_1^1 in their definition does not actually alter anything!). In the second case the functions vanish on the boundary.

The spatial finite element semidiscretization of Problem 2.1.3 is obtained from (2.13), by a "replacement" of the appropriate spaces.

2.5.3 Problem (Finite elements for Cauchy-Dirichlet)**.** *Let $\tilde{g}_h(t) \in \mathbb{V}_h^\ell$ be an* interpolation *of $\tilde{g}(t)$ (the extension of $g(t)$ introduced in 2.3.1). Find $u_h \in \mathrm{C}^1([0,T];\mathbb{V}_h^\ell)$ such that:*

$$u_h(t) - \tilde{g}_h(t) \in \mathring{\mathbb{V}}_h^\ell, \tag{2.25}$$

$$\int_\Omega \frac{\partial_t u_h}{Qu_h}\phi_h + \frac{\nabla u_h}{Qu_h}\nabla\phi_h \,\mathrm{d}x = \int_\Omega f\phi_h \,\mathrm{d}x, \quad \forall t \in [0,T], \quad \forall \phi_h \in \mathring{\mathbb{V}}_h^\ell. \tag{2.26}$$

The existence, uniqueness and apriori error estimates of the finite element solution u_h to Problem (2.5.3) are discussed in [DD00].

Chapter 3

Aposteriori error analysis for the mean curvature flow of graphs

This is the central chapter of the dissertation; its main goal will be to understand the relationship between the exact MCF of graphs, described by the solution u of Problem 2.1.3, and its finite element approximation, described by the solution u_h of Problem 2.5.3.

We will derive *aposteriori bounds for the error* between u_h and u in certain norm-like quantities. We consider general right-hand side f and time-dependent boundary values g. One of the two main purposes for deriving aposteriori error bounds is to have a computable control over the numerical error, as all the quantities appearing in the bound depend only on the data and the approximate solution u_h.

Problem 2.5.3 has been analyzed by Dziuk [Dzi99] from the apriori viewpoint. He established an *apriori error bound*, that is in terms of quantities that depend on the exact solution u. That bound, valid under rather strong regularity assumptions on u, implies the convergence of u_h to u, as $h \to 0$, with order h in certain norm-like quantities. His proof is limited to homogeneous right-hand side

$f = 0$ and time-independent boundary data g.

Our situation contrasts with (or rather complements) that situation, since the aposteriori constants themselves depend on the approximate solution u_h, and are numerically computable if needed and do not require so strong regularity assumptions on the exact solution (although such assumptions would improve them).

As a by-product of our aposteriori analysis we also obtain a finer understanding of the constants that are involved in the apriori analysis, and their dependence on the exact solution. (By "constant" here we refer to C in an inequality of the type error $\leq C$estimate.) The worst case scenario must be included in the analysis and the main technique for proving these bounds is the Gronwall inequality — a linear technique applied to a nonlinear problem — so the behavior of these constants can be very wild. Assuming we can compute exactly the constants appearing in the approximation properties of the interpolation operators that will be used, the *constants appearing in the aposteriori bound can be computed*, if we wish to.

3.1 How to measure the error

In any error analysis it is crucial to find what is the best concept of error that fits the problem. By a concept of error we loosely mean a norm, or a metric, or any measure of how close is the approximate solution to the exact solution in an appropriate sense.

In finite elements for elliptic and parabolic problems, due to the variational nature of most problems that are treated it is customary to use Sobolev norms to measure the error. In linear problems L_2 based Sobolev norms are naturally

related to the *energy norm* which is in turn related to the nature of the differential operator. The extension of these norms to handle nonlinear problems has sometimes to be made carefully. For instance in some cases, the nature of the problem implies the use of L_p spaces with $p \neq 2$.

Here we are dealing with a highly nonlinear problem and we encounter serious difficulties in using Sobolev norms. The main problem is to relate Sobolev norms to quantities that can be naturally extracted from the problem, like the energy estimate of Section 2.4. This leads us to look for a concept of error that is more appropriate to our problem. This leads us to introduce the geometric error.

3.1.1 Definition (Geometric error)**.** Let u be the solution of Problem 2.1.3 and u_h be the finite element solution give by Problem 2.5.3. For each $t \in [0, T]$, define

$$A(t) := \int_\Omega |Nu_h(x,t) - Nu(x,t)|^2 \, Qu(x,t) \, \mathrm{d}x \tag{3.1}$$

$$B(t) := \int_0^t \int_\Omega \left(Vu_h(x,t) - Vu(x,t)\right)^2 Q(x,t) u \, \mathrm{d}x \, \mathrm{d}t \tag{3.2}$$

The real valued functions A and B are the building blocks of the *geometric error*:

$$\begin{aligned} B(t) + \sup_{[0,t]} A(s) = & \int_0^t \int_\Omega \left(Vu_h - Vu\right)^2 Qu \, \mathrm{d}x \, \mathrm{d}s \\ & + \sup_{(0,t)} \int_\Omega |Nu_h - Nu|^2 \, Qu \, \mathrm{d}x. \end{aligned} \tag{3.3}$$

for all $t \in [0, T]$.

It's quite apparent that the quantities measuring the error between the approximate and the exact solution are *not* usual (Sobolev) norms. These are not even metrics, since the terms are not symmetric.

The nature of these quantities is geometric as they are related to the structure of the parabolic operator at hand, the integrals of the form $\int_\Omega \cdot\, Qu \,\mathrm{d}x$ in (3.3) are just integrals over the surface $\Gamma(t)$ which give us the $\mathrm{L}_2(\Gamma)$ norm of the *difference of normals* and the *difference of normal velocities*. A comparison with the integrals appearing in the left-hand side of (2.20) explains in part why they "fit" the problem.

It is also worth stressing that, despite our concept of error being naturally related to MCF of graphs, it hasn't been used in the literature for aposteriori error control of parabolic equations. In fact, the geometric nature contrasts sharply with the pure analytic setting found in Verfürth's monograph [Ver98]. Geometric quantities similar to the one we use are employed by Fierro & Veeser in their work on the nonparametric prescribed mean curvature equation [FV02]. Owing to the elliptic nature of their problem they are able to introduce symmetric versions of these quantities that are more manageable. Unfortunately, in our case the use of symmetric quantities doesn't seem to lead to any reasonable aposteriori error bound and we have to use non-symmetric ones.

3.2 Basic geometry

In this section we present some simple relations among geometric quantities that will be instrumental in the derivation of the main results.

We begin with an inequality relating vectors in $\mathbb{R}^{d-1}$ and vectors in $\mathbb{R}^d$.

3.2.1 Lemma (Fierro-Veeser inequality [FV02])**.** *Suppose* $\boldsymbol{p}_1, \boldsymbol{p}_2 \in \mathbb{R}^d$. *Let* $\widetilde{\boldsymbol{p}}_i := (\boldsymbol{p}_i; -1) \in \mathbb{R}^{d+1}$, $q_i := |\widetilde{\boldsymbol{p}}_i|$ $(= (1 + |\boldsymbol{p}_i|^2)^{1/2})$ *and* $\boldsymbol{n}_i := \widetilde{\boldsymbol{p}}_i / q_i$ *for* $i = 1, 2$.

Then

$$|\boldsymbol{p}_1 - \boldsymbol{p}_2| \, \frac{1}{q_1^2} \leq 2 \, |\boldsymbol{n}_1 - \boldsymbol{n}_2| + |\boldsymbol{n}_1 - \boldsymbol{n}_2|^2 \, q_2. \tag{3.4}$$

Proof Although this proof was given by Fierro & Veeser [FV02], we include it for the sake of completeness.

Start with the simple bound

$$\begin{aligned} |\boldsymbol{p}_1 - \boldsymbol{p}_2| = |\widetilde{\boldsymbol{p}}_1 - \widetilde{\boldsymbol{p}}_2| &= \left| \widetilde{\boldsymbol{p}}_1 - \frac{q_1}{q_2} \widetilde{\boldsymbol{p}}_2 + (q_1 - q_2) \, \frac{\widetilde{\boldsymbol{p}}_2}{q_2} \right| \\ &\leq |\boldsymbol{n}_1 - \boldsymbol{n}_2| \, q_1 + |q_1 - q_2| \, . \end{aligned}$$

Multiply this equation by $1/q_1^2$, and control the last term by observing that

$$\begin{aligned} |q_1 - q_2| \, \frac{1}{q_1^2} &= \left| \frac{1}{q_1} - \frac{q_2}{q_1^2} + \frac{1}{q_2} - \frac{1}{q_2} + \frac{1}{q_1} - \frac{1}{q_1} \right| \\ &\leq \left| \frac{1}{q_1} - \frac{1}{q_2} \right| + \left| \frac{1}{q_1} \left(1 - \frac{q_2}{q_1} \right) - \frac{1}{q_2} \left(-\frac{q_2}{q_1} + 1 \right) \right| \\ &= \left| \frac{1}{q_1} - \frac{1}{q_2} \right| + \left| \frac{1}{q_1} - \frac{1}{q_2} \right|^2 q_2 \\ &\leq |\boldsymbol{n}_1 - \boldsymbol{n}_2| + |\boldsymbol{n}_1 - \boldsymbol{n}_2|^2 \, q_2, \end{aligned}$$

where the last step we have use the fact that $1/q_i$ is the last component of the vector $\boldsymbol{n}_i$. Piecing together, and recalling that $q_1 \geq 1$ we obtain the result. □

3.2.2 Lemma. *With the same notation as Lemma 3.2.1 the following relations hold:*

$$1 - \frac{1 + \boldsymbol{p}_1 \cdot \boldsymbol{p}_2}{q_1 q_2} = \frac{1}{2} \, |\boldsymbol{n}_1 - \boldsymbol{n}_2|^2 \, , \tag{3.5}$$

$$\left| \left(\frac{1}{q_1} - \frac{1}{q_2} \right) \left(\frac{\boldsymbol{p}_1}{q_1} - \frac{\boldsymbol{p}_2}{q_2} \right) \right| \leq \frac{1}{2} \, |\boldsymbol{n}_1 - \boldsymbol{n}_2|^2 \, , \tag{3.6}$$

$$\frac{|\boldsymbol{p}_1 - \boldsymbol{p}_2|}{q_1} \leq (1 + |\boldsymbol{p}_2|) \, |\boldsymbol{n}_1 - \boldsymbol{n}_2| \, . \tag{3.7}$$

Proof The identity (3.5) is a direct consequence of the definitions:

$$\begin{aligned}|\boldsymbol{n}_1 - \boldsymbol{n}_2|^2 &= \left|\frac{(\boldsymbol{p}_1; -1)}{q_1} - \frac{(\boldsymbol{p}_2; -1)}{q_2}\right|^2 \\ &= 2 - 2\,\frac{\boldsymbol{p}_1 \cdot \boldsymbol{p}_2 + 1}{q_1 q_2}.\end{aligned}$$

The inequality (3.6) is just Young inequality applied to the last component and the first d components of the vector $\boldsymbol{n}_1 - \boldsymbol{n}_2$:

$$\begin{aligned}\left|\frac{1}{q_1} - \frac{1}{q_2}\right| \left|\frac{\boldsymbol{p}_1}{q_1} - \frac{\boldsymbol{p}_2}{q_2}\right| &\leq \frac{1}{2}\left|\frac{1}{q_1} - \frac{1}{q_2}\right|^2 + \frac{1}{2}\left|\frac{\boldsymbol{p}_1}{q_1} - \frac{\boldsymbol{p}_2}{q_2}\right|^2 \\ &= \frac{1}{2}\,|\boldsymbol{n}_1 - \boldsymbol{n}_2|^2\,.\end{aligned}$$

As for (3.7) it is easily derived as follows

$$\begin{aligned}\left|\frac{\boldsymbol{p}_1}{q_1} - \frac{\boldsymbol{p}_2}{q_1}\right| &= \left|\frac{\boldsymbol{p}_1}{q_1} - \frac{\boldsymbol{p}_2}{q_2} + \frac{\boldsymbol{p}_2}{q_2} - \frac{\boldsymbol{p}_2}{q_1}\right| \\ &\leq |\boldsymbol{n}_1 - \boldsymbol{n}_2| + \left|\frac{1}{q_2} - \frac{1}{q_1}\right| |\boldsymbol{p}_2| \\ &\leq |\boldsymbol{n}_1 - \boldsymbol{n}_2|\,(1 + |\boldsymbol{p}_2|).\end{aligned}$$

This concludes our proof. □

3.3 The residual and the error equation

Throughout this chapter we will be using the following notation:

3.3.1 Definition (Notation for integral representation and duality pairing)**.** Given two functions v and w such that their product is in $\mathrm{L}_1(D)$, (D, μ) being a given measure space, we write

$$\langle v, w\rangle_D = \int_D v(x)w(x)\,\mathrm{d}\mu x. \tag{3.8}$$

If $D = \Omega$ we omit the subscript in the left-hand side. The only two measures we will use are the Lebesgue measure, denoted simply by d in the integral, and the codimension 1 (Hausdorff) measure denoted by $\mathrm{s(d)}$ in the integral. The choice of the set D should imply clearly which measure we are dealing with.

In this chapter we also need to refer to the pairing of a linear functional $\mathscr{F}$ acting on a function v in its domain X. For this we use a modification of (3.8) and denote the *duality pairing* operation by

$$\langle \mathscr{F} \,|\, v \rangle \,. \tag{3.9}$$

We say that the linear functional $\mathscr{F}$ *admits a representation* as a function if we can write

$$\langle \mathscr{F} \,|\, v \rangle = \sum_{i=1}^{k} \langle f_i, v \rangle_{D_i} \tag{3.10}$$

for suitable functions f_i and measure spaces D_i. Since we are dealing with only two measures in our case k is at most 2.

Before starting our discussion on aposteriori bounds for the MCF, we point out that the residual estimation energy technique that we will employ can be applied to the simpler situation of the heat equation. This leads to aposteriori error estimates for the heat equation that were not present in the literature to the best of our knowledge. The result has been hence included in Section A.3. Since the case of the heat equation entails fewer details than the MCF case, reading it before proceeding here might prove helpful (to be sure, one should compare Section 3.5 with Section A.3).

If (2.26) is tested with any function $\phi \in \overset{\circ}{\mathrm{W}}{}^1_1(\Omega)$ (instead of a finite element function $\phi_h \in \overset{\circ}{\mathbb{V}}{}^\ell_h$) and then subtracted from (2.13) with the same test function,

we obtain a definition of the *residual functional*

$$\langle \mathscr{R} \,|\, \phi \rangle := \left\langle \frac{\partial_t u_h}{Q u_h} - \frac{\partial_t u}{Q u}, \phi \right\rangle + \left\langle \frac{\nabla u_h}{Q u_h} - \frac{\nabla u}{Q u}, \nabla \phi \right\rangle . \tag{3.11}$$

The functional $\mathscr{R}$ is time dependent and $\mathscr{R}(t) \in \mathrm{W}_1^{-1}(\Omega)$, the dual space of $\overset{\circ}{\mathrm{W}}{}_1^1(\Omega)$, for all $t \in [0, T]$.

The starting point of our residual based aposteriori estimation, is to observe that the residual functional vanishes on $\overset{\circ}{\mathbb{V}}{}_h^\ell$. This is the so called *Galerkin orthogonality* property, which yields the error equation

$$\langle \mathscr{R} \,|\, \phi \rangle = \langle \mathscr{R} \,|\, \phi - \phi_h \rangle = \left\langle \frac{\partial_t u_h}{Q u_h} - f, \phi - \phi_h \right\rangle + \left\langle \frac{\nabla u_h}{Q u_h}, \nabla(\phi - \phi_h) \right\rangle , \tag{3.12}$$

for all $\phi_h \in \overset{\circ}{\mathbb{V}}{}_h^\ell$.

An integration by parts in the space variable leads to the representation of the residual functional as

$$\begin{aligned} \langle \mathscr{R} \,|\, \psi \rangle &= \langle r, \psi \rangle + \langle j, \psi \rangle_{\Sigma_h} \\ &:= \left\langle \frac{\partial_t u_h}{Q u_h} - f - \operatorname{div} \left(\frac{\nabla u_h}{Q u_h} \right), \psi \right\rangle + \left\langle \left[\!\!\left[\frac{\nabla u_h}{Q u_h} \right]\!\!\right], \psi \right\rangle_{\Sigma_h} , \end{aligned} \tag{3.13}$$

for any $\psi \in \overset{\circ}{\mathrm{W}}{}_1^1(\Omega)$. Here $\Sigma_h := \bigcup_{\mathscr{S}_h^\circ} S$, with $\mathscr{S}_h^\circ$ being the set of internal edges (or faces) of the triangulation $\mathscr{T}_h$, and j is the *jump residual* defined as the jump of the field $\nabla u_h / Q u_h$. The *jump of a vector field* $\boldsymbol{\psi}$ across a $d-1$ dimensional smooth manifold M is defined by

$$[\![\boldsymbol{\psi}]\!]_M (x) = \lim_{\varepsilon \to 0} \left(\boldsymbol{\psi}(x + \varepsilon \boldsymbol{\nu}(x)) - \boldsymbol{\psi}(x - \varepsilon \boldsymbol{\nu}(x)) \right) \cdot \boldsymbol{\nu}(x) \tag{3.14}$$

for $x \in M$, here $\boldsymbol{\nu}(x)$ is a unit length vector orthogonal to M at the point x. This definition is independent on the orientation of the vector $\boldsymbol{\nu}$, and valid for vector fields that are discontinuous on the manifold M. The function r appearing in (3.13) is referred to as the *interior residual*.

Choice of the test function

In order to exploit (3.12) for obtaining an a posteriori error estimate, it is convenient to choose

$$\phi(x,t) := \partial_t e(x,t); \tag{3.15}$$

$$e(x,t) := u_h(x,t) - u(x,t); \tag{3.16}$$

$$\phi_h(x,t) = I_h \phi(x,t). \tag{3.17}$$

The operator I_h could be any suitable interpolation operator from $\mathrm{W}_1^1(\Omega)$ onto $\mathbb{V}_h^\ell$. We choose I_h to be the Scott-Zhang interpolator of Theorem A.2.3. In order for us to employ $\partial_t e$ as a test function we must have $\partial_t e \in \overset{\circ}{\mathrm{W}}{}_1^1$. This motivates the following

3.3.2 Hypothesis (Exact boundary data resolution)**.** *We assume either:*

(a) that the boundary value g is approximated exactly by g_h.

or

(b) that g is time independent.

For what follows we will assume that this is the case to simplify the analysis. Notice that *we will remove this assumption* in the last Section 3.7 and show how to treat boundary data.

3.4 Estimating the left-hand side of the error equation

We estimate now the left-hand side of (3.12) using (3.11). The first term is handled through the following inequality.

3.4.1 Lemma (Velocity term)**.** *Let*

$$\varrho_1(t) := \frac{1}{2} \left\| \partial_t u_h(t) \right\|^2_{\mathrm{L}_\infty(\Omega)}, \tag{3.18}$$

we have

$$\left\langle \frac{\partial_t u_h}{Q u_h} - \frac{\partial_t u}{Q u}, \partial_t u_h - \partial_t u \right\rangle \geq \frac{1}{2} \mathrm{d}_t B(t) - \varrho_1 A(t). \tag{3.19}$$

Proof

$$\begin{aligned}
&\left\langle \frac{\partial_t u_h}{Q u_h} - \frac{\partial_t u}{Q u}, \partial_t u_h - \partial_t u \right\rangle \\
&= \int_\Omega (V u_h - V u)^2 Q u + \int_\Omega \partial_t u_h \left(\frac{1}{Q u} - \frac{1}{Q u_h} \right) (V u_h - V u) Q u \\
&\geq \mathrm{d}_t B(t) - \left\| \partial_t u_h \right\|_{\mathrm{L}_\infty(\Omega)} \int_\Omega \left| \frac{1}{Q u} - \frac{1}{Q u_h} \right| \sqrt{Q u} \left| V u_h - V u \right| \sqrt{Q u} \\
&\geq \mathrm{d}_t B(t) - \left\| \partial_t u_h \right\|_{\mathrm{L}_\infty(\Omega)} \left(\int_\Omega \left| N u_h - N u \right|^2 Q u \right)^{1/2} \left(\int_\Omega (V u_h - V u)^2 Q u \right)^{1/2} \\
&\geq \mathrm{d}_t B(t) - \frac{1}{2} \mathrm{d}_t B(t) - \varrho_1(t) A(t) \\
&= \frac{1}{2} \mathrm{d}_t B(t) - \varrho_1 A(t)
\end{aligned}$$

□

In order to estimate the second term in (3.12) we will use the following identity.

3.4.2 Lemma (Dziuk identity[Dzi99]). *If v and w be differentiable functions on $\Omega \times (0,T)$, then*

$$\begin{aligned}\frac{1}{2}\partial_t\left(|Nv-Nw|^2 Qw\right) = &\left(\frac{\nabla v}{Qv}-\frac{\nabla w}{Qw}\right)\cdot\nabla\left(\partial_t v-\partial_t w\right)\\ &-\nabla\partial_t v\cdot\left(\frac{\nabla w}{Qv}-\frac{\nabla w}{Qw}+\frac{\nabla v}{Qv}-\frac{1+\nabla w\cdot\nabla v}{(Qv)^2}\frac{\nabla v}{Qv}\right)\end{aligned} \tag{3.20}$$

Proof This identity, only claimed in [Dzi99], deserves a derivation. In light of the geometric relation (3.5), we can write

$$\begin{aligned}\frac{1}{2}\partial_t\left(|Nw-Nv|^2 Qw\right) =&\partial_t\left(\left(1-\frac{1+\nabla w\cdot\nabla v}{QwQv}\right)Qw\right)\\ =&\partial_t\left(Qw-\frac{1+\nabla w\cdot\nabla v}{Qv}\right).\end{aligned}$$

Calculating each term separately we get

$$\partial_t Qw = \frac{\nabla w\cdot\partial_t\nabla w}{Qw}; \tag{3.21}$$

$$\partial_t\frac{1}{Qv} = -\frac{\nabla v\cdot\partial_t\nabla v}{(Qv)^3} \tag{3.22}$$

and

$$\partial_t\left(1+\nabla w\cdot\nabla v\right) = \partial_t\nabla w\cdot\nabla v+\nabla w\cdot\partial_t\nabla v. \tag{3.23}$$

It follows that

$$\begin{aligned}\frac{1}{2}\partial_t\left(|Nw-Nv|^2 Qw\right) =&\frac{\nabla w}{Qw}\cdot\partial_t\nabla w-\frac{\nabla v}{Qv}\cdot\partial_t\nabla w\\ &-\frac{\nabla w\cdot\partial_t\nabla v}{Qv}+(1+\nabla w\cdot\nabla v)\frac{\nabla v\cdot\partial_t\nabla v}{(Qv)^3}.\end{aligned}$$

By subtracting and adding

$$\frac{\nabla w}{Qw}\cdot\partial_t\nabla v$$

in the right-hand side above, isolating

$$\left(\frac{\nabla v}{Qv} - \frac{\nabla w}{Qw}\right) \cdot \nabla \left(\partial_t v - \partial_t w\right) \tag{3.24}$$

and collecting all the remaining terms we obtain (3.20). □

We can now state and prove an inequality concerning the term with gradients.

3.4.3 Lemma (Normals and gradients)**.** *Let*

$$\varrho_2(t) := \|\nabla \partial_t u_h(t)\|_{\mathrm{L}_\infty(\Omega)}\,. \tag{3.25}$$

Then

$$\left\langle \frac{\nabla u_h}{Qu_h} - \frac{\nabla u}{Qu}, \nabla(\partial_t u_h - \partial_t u) \right\rangle \geq \frac{1}{2}\,\mathrm{d}_t A(t) - \varrho_2(t) A(t) \tag{3.26}$$

Proof In view of (3.20) (3.5) we start with

$$\begin{aligned}
&\left\langle \frac{\nabla u_h}{Qu_h} - \frac{\nabla u}{Qu}, \nabla(\partial_t u_h - \partial_t u) \right\rangle = \frac{1}{2}\,\mathrm{d}_t A(t) \\
&- \int_\Omega \nabla \partial_t u_h \cdot \left(\frac{\nabla u}{Qu_h} - \frac{\nabla u}{Qu} - \frac{\nabla u_h}{Qu_h} - \frac{1 + \nabla u \cdot \nabla u_h}{Q^2 u_h} \frac{\nabla u_h}{Qu_h} \right).
\end{aligned}$$

The last term above can be split by adding and subtracting $(Qu\nabla u_h)/(Qu_h)^2$ as follows

$$\begin{aligned}
&- \int_\Omega \nabla \partial_t u_h \cdot \left(\frac{\nabla u}{Qu_h} - \frac{\nabla u}{Qu} + \frac{\nabla u_h}{Qu_h} - \frac{Qu \nabla u_h}{(Qu_h)^2} \right) \\
&- \int_\Omega \nabla \partial_t u_h \cdot \left(\frac{Qu \nabla u_h}{(Qu_h)^2} - \frac{1 + \nabla u \cdot \nabla u_h}{Q^2 u_h} \frac{\nabla u_h}{Qu_h} \right).
\end{aligned}$$

We now estimate the absolute values of these terms. The first term with integral sign above is bounded with the use of (3.6) as follows

$$\begin{aligned}
&\int_\Omega \nabla \partial_t u_h \cdot \left(\frac{\nabla u}{Qu_h} - \frac{\nabla u}{Qu} + \frac{\nabla u_h}{Qu_h} - \frac{Qu \nabla u_h}{(Qu_h)^2} \right) \\
&\qquad \leq \|\nabla \partial_t u_h\|_{\mathrm{L}_\infty(\Omega)} \int_\Omega \left| \left(\frac{1}{Qu} - \frac{1}{Qu_h} \right) \left(\frac{\nabla u_h}{Qu_h} - \frac{\nabla u}{Qu} \right) Qu \right| \\
&\qquad \leq \varrho_2(t) \frac{1}{2} A(t).
\end{aligned}$$

The second term with integral sign is bounded by applying again (3.5) as follows

$$\int_\Omega \nabla\partial_t u_h \cdot \left(\frac{\nabla u_h}{(Qu_h)^2} Qu - \frac{1+\nabla u\cdot\nabla u_h}{Q^2 u_h}\frac{\nabla u_h}{Qu_h}\right) \tag{3.27}$$

$$\leq \|\nabla\partial_t u_h\|_{\mathrm{L}_\infty(\Omega)} \int_\Omega \left| \left(1 - \frac{1+\nabla u_h\cdot\nabla u}{Qu_h Qu}\right) Qu \frac{\nabla u_h}{(Qu_h)^2}\right| \tag{3.28}$$

$$\leq \varrho_2(t)\frac{1}{2}A(t). \tag{3.29}$$

The assertion of the lemma is easily obtained. □

3.4.4 Lemma (Estimate of the geometric terms)**.** *Define*

$$\varrho(t) := \varrho_1(t) + \varrho_2(t).$$

Then

$$\begin{aligned} A(t) + B(t) \leq & A(0) + 2\int_0^t \varrho(s)A(s)\,\mathrm{d}s \\ & + 2\int_0^t \langle \mathscr{R}(s) \,|\, \partial_t\left(e(s) - I_h e(s)\right)\rangle \,\mathrm{d}s. \end{aligned} \tag{3.30}$$

Proof Replacing (3.19) and (3.26) in (3.12), we obtain

$$\frac{1}{2}\left(\,\mathrm{d}_t A(t) + \,\mathrm{d}_t B(t)\right) \leq \langle \mathscr{R} \,|\, \partial_t e(t) - I_h\partial_t e(t)\rangle + \varrho(t)A(t), \tag{3.31}$$

for all $t \in [0,T]$. An integration in time over the interval $[0,t]$ yields the desired result. □

3.5 Residual estimate

We now estimate the integral of the residual term appearing in the right-hand side of (3.30). Let us denote by $d' = d/(d-1)$ the conjugate exponent of the dimension d.

3.5.1 Remark (Scott-Zhang interpolation and the Fierro-Veeser geometric inequality)**.** We will use the following properties of the Scott-Zhang interpolator, cf. Theorem A.2.3 and corollary A.2.4:

$$\|\psi - I_h\psi\|_{\mathrm{L}_{d'}(K)} \leq C_1 \, |\psi|_{\mathrm{W}^1_1(\mathscr{U}_K^h)}\,, \tag{3.32}$$

$$\|\psi - I_h\psi\|_{\mathrm{L}_1(\partial K)} \leq 2C_2 \, |\psi|_{\mathrm{W}^1_1(\mathscr{U}_K^h)} \tag{3.33}$$

where $\mathscr{U}_K^h$ is the neighborhood of the element K in the triangulation $\mathscr{T}_h$, that is

$$\mathscr{U}_K^h = \bigcup \{K' \in \mathscr{T}_h : \; K' \cap K \neq \emptyset\}\,. \tag{3.34}$$

We use these rather unusual estimates for the Scott-Zhang interpolant because we wish $\sqrt{A(t)}$ to appear on the right-hand side.

Ideally we would like to bound $|\nabla u_h - \nabla u|^2$ from above by $C[u_h]\,|Nu_h - Nu|^2\,Qu$, with a constant $C[u_h]$ independent of u (think of u_h being unrelated to u in this paragraph). That is, we need a geometric relation of the type

$$\frac{|\boldsymbol{p}_1 - \boldsymbol{p}_2|^2}{\kappa(\boldsymbol{p}_1)\,|\boldsymbol{n}_1 - \boldsymbol{n}_2|^2\,q_2} \leq C, \tag{3.35}$$

where we used the notation of Lemma 3.2.1 and κ is some function. But this is not possible because if we fix $\boldsymbol{p}_1$, we observe that $\boldsymbol{n}_1 - \boldsymbol{n}_2$ is bounded and we let $|\boldsymbol{p}_2| \to \infty$ we obtain

$$\frac{|\boldsymbol{p}_1 - \boldsymbol{p}_2|^2}{\kappa(\boldsymbol{p}_1)\,|\boldsymbol{n}_1 - \boldsymbol{n}_2|^2\,q_2} \geq C\frac{|\boldsymbol{p}_1 - \boldsymbol{p}_2|^2}{q_2} = \mathrm{O}(|\boldsymbol{p}_2|) \to \infty. \tag{3.36}$$

This difficulty is circumvented by using the L_1 norm and the Fierro-Veeser inequality given in Lemma 3.2.1 which reads

$$|\nabla u_h - \nabla u| = Q^2 u_h \frac{|\nabla u_h - \nabla u|}{Q^2 u_h} \leq Q^2 u_h \left(2\,|Nu_h - Nu| + |Nu_h - Nu|^2\,Qu\right). \tag{3.37}$$

Notice that the last term is the "price to pay". Indeed, such a term is cumbersome since the power is too high, this will yield a term of the form $\gamma A(t)$ on the right-hand side (where γ is some coefficient) which has to be dealt with.

In the sequel we will need the definition of local indicators and global estimators.

3.5.2 Definition (Local indicators and weights)**.** To each simplex $K \in \mathscr{T}_h$ we can associate the following *local indicators*:

$$\textit{parabolic}: \qquad \eta_1^K(t) := h_K^{d/2} \left(C_1 \left\| \partial_t r(t) \right\|_{\mathrm{L}_d(K)} + C_2 \left\| \partial_t j(t) \right\|_{\mathrm{L}_\infty(\partial K)} \right). \tag{3.38}$$

$$\textit{elliptic}: \qquad \eta_0^K(t) := h_K^{d/2} \left(C_1 \left\| r(t) \right\|_{\mathrm{L}_d(K)} + C_2 \left\| j(t) \right\|_{\mathrm{L}_\infty(\partial K)} \right); \tag{3.39}$$

and the following *local weights*:

$$\omega_K(t) := \sup_{x \in \mathscr{U}_K^h} Q^2 u_h(x,t); \tag{3.40}$$

$$\alpha_K(t) := \omega_K(t)^2 \sup_{x \in \mathscr{U}_K^h} \frac{1}{Qu(x,t)}; \tag{3.41}$$

Let us introduce the following

3.5.3 Definition (Global error estimators)**.** Using the local indicators of Definition 3.5.2, and two constants M and γ that depend only on the shape regularity σ_0 of the triangulation (see the proof of Lemma 3.5.4 for details on M and γ). we introduce the following *error estimators*:

$$\textit{elliptic}: \qquad \mathscr{E}_{2,0}(t)^2 := \gamma^2 \sum_{K \in \mathscr{T}_h} \alpha_K(t) \eta_0^K(t)^2, \tag{3.42}$$

$$\textit{parabolic}: \qquad \mathscr{E}_{2,1}(t) := \int_0^t \dot{\mathscr{E}}_{2,1}(s)\, \mathrm{d}s, \tag{3.43}$$

$$\dot{\mathscr{E}}_{2,1}(t)^2 := \gamma^2 \sum_{K \in \mathscr{T}_h} \alpha_K(s) \eta_1^K(s)^2,$$

$$\text{(3.44)}\quad \textit{elliptic conditional}: \qquad \mathscr{E}_{\infty,0}(t) := M \max_{K\in\mathscr{T}_h} \omega_K(t)\eta_0^K(t)h_K^{-d/2},$$

$$\text{(3.45)}\quad \textit{parabolic conditional}: \quad \mathscr{E}_{\infty,1}(t) := \int_0^t \dot{\mathscr{E}}_{\infty,1}(s)\,\mathrm{d}s$$

$$\dot{\mathscr{E}}_{\infty,1}(t) := M \max_{K\in\mathscr{T}_h} \omega_K(t)\eta_1^K(t)h_K^{-d/2}.$$

$$\text{(3.46)}\quad \textit{initial}: \qquad \mathscr{E}_0^2 := (1+2\mathscr{E}_{\infty,0}(0))A(0) + 2\mathscr{E}_{2,0}(0)\sqrt{A(0)}$$

3.5.4 Lemma (Residual estimate)**.** *For each $t\in[0,T]$, the following inequality is verified*

$$\begin{aligned} A(t)+B(t) \leq & \mathscr{E}_0^2 + 2\mathscr{E}_{2,0}(t)A(t)^{1/2} + 2\mathscr{E}_{\infty,0}A(t) \\ & + 2\int_0^t \dot{\mathscr{E}}_{2,1}(s)A(s)^{1/2}\,\mathrm{d}s + 2\int_0^t \dot{\mathscr{E}}_{\infty,1}(s)A(s)\,\mathrm{d}s \\ & + 2\int_0^t \varrho(s)A(s)\,\mathrm{d}s. \end{aligned} \tag{3.47}$$

Proof An application of the representation of the residual (3.13), the integration by parts in time, and the commutativity property $\partial_t I_h = I_h\partial_t$ yield

$$\begin{aligned} &\int_0^t \langle \mathscr{R}(s) \,|\, \partial_t\left(e(s) - I_h e(s)\right)\rangle \,\mathrm{d}s \\ &\quad = \int_0^t \left(\langle r(s), \partial_t(e(s)-I_he(s))\rangle + \langle j(s), \partial_t(e(s)-I_he(s))\rangle_{\Sigma_h}\right)\,\mathrm{d}s \\ &\quad = \left[\langle r(s), e(s)-I_he(s)\rangle + \langle j(s), e(s)-I_he(s)\rangle_{\Sigma_h}\right]_{s=0}^{s=t} \\ &\quad -\int_0^t \langle \partial_t r(s), e(s)-I_he(s)\rangle + \langle \partial_t j(s), e(s)-I_he(s)\rangle_{\Sigma_h}\mathrm{d}s \\ &\quad \leq \sum_{K\in\mathscr{T}_h} \Bigg(\|r(t)\|_{\mathrm{L}_d(K)} \|e(t)-I_he(t)\|_{\mathrm{L}_{d'}(K)} + \|r(0)\|_{\mathrm{L}_d(K)} \|e(0)-I_he(0)\|_{\mathrm{L}_{d'}(K)} \\ &\quad + \frac{1}{2}\|j(t)\|_{\mathrm{L}_\infty(\partial K)} \|e(t)-I_he(t)\|_{\mathrm{L}_1(\partial K)} + \frac{1}{2}\|j(0)\|_{\mathrm{L}_\infty(\partial K)} \|e(0)-I_he(0)\|_{\mathrm{L}_1(\partial K)} \\ &\quad + \int_0^t \Big(\|\partial_t r(s)\|_{\mathrm{L}_d(K)} \|e(s)-I_he(s)\|_{\mathrm{L}_{d'}(K)} \\ &\quad + \frac{1}{2}\|\partial_t j(s)\|_{\mathrm{L}_\infty(\partial K)} \|e(s)-I_he(s)\|_{\mathrm{L}_1(\partial K)}\Big)\,\mathrm{d}s\Bigg) \end{aligned}$$

In view of the interpolation properties of the Scott-Zhang interpolator (3.32) and (3.33), we obtain

$$\begin{aligned}
&\int_0^t \langle \mathscr{R}(s) \,|\, \partial_t \left(e(s) - I_h e(s)\right)\rangle \,\mathrm{d}s \\
&\qquad \leq \sum_{K\in\mathscr{T}_h} \Bigg(\eta_0^K(t) \left\|\nabla e(0)\right\|_{\mathrm{L}_1(\mathscr{U}_K^h)} + \eta_0^K(t) \left\|\nabla e(t)\right\|_{\mathrm{L}_1(\mathscr{U}_K^h)} \\
&\qquad\qquad + \int_0^t \eta_1^K(s) \left\|\nabla e(s)\right\|_{\mathrm{L}_1(\mathscr{U}_K^h)} \,\mathrm{d}s \Bigg).
\end{aligned} \tag{3.48}$$

Inequality (3.37) implies

$$\begin{aligned}
\left\|\nabla e(t)\right\|_{\mathrm{L}_1(\Omega')} &= \int_{\Omega'} |\nabla(u_h - u)| \leq \int_{\Omega'} Q^2 u_h \frac{|\nabla(u_h - u)|}{Q^2 u_h} \\
&\leq \sup_{\Omega'} Q^2 u_h \left(\int_{\Omega'} 2 \left|Nu_h - Nu\right| \sqrt{Qu} \frac{1}{\sqrt{Qu}} + \left|Nu_h - Nu\right|^2 Qu \right),
\end{aligned} \tag{3.49}$$

for any $\Omega' \subset \Omega$.

For the remainder of this section introduce the shorthand

$$\mathscr{N} := \left|Nu_h - Nu\right| \sqrt{Qu} \tag{3.50}$$

We continue our bound in (3.48) by using (3.49):

$$\begin{aligned}
&\int_0^t \langle \mathscr{R}(s) \,|\, \partial_t e(s) - I_h \partial_t e(s)\rangle \,\mathrm{d}s \\
&\qquad \leq \sum_{K\in\mathscr{T}_h} \eta_0^K(0) h_K^{-d/2} \omega_K(0) \int_{\mathscr{U}_K^h} \left(\frac{2\mathscr{N}(0)}{\sqrt{Qu(0)}} + \mathscr{N}(0)^2 \right) \\
&\qquad + \sum_{K\in\mathscr{T}_h} \eta_0^K(t) h_K^{-d/2} \omega_K(t) \int_{\mathscr{U}_K^h} \left(\frac{2\mathscr{N}(t)}{\sqrt{Qu(t)}} + \mathscr{N}(t)^2 \right) \\
&\qquad + \sum_{K\in\mathscr{T}_h} \int_0^t \eta_1^K(s) h_K^{-d/2} \omega_K(s) \int_{\mathscr{U}_K^h} \left(\frac{2\mathscr{N}(s)}{\sqrt{Qu(s)}} + \mathscr{N}(s)^2 \right) \mathrm{d}s.
\end{aligned} \tag{3.51}$$

The first two terms can be bounded by using the following (take $t = 0$ for the

first term)

$$\sum_{K\in\mathscr{T}_h} \eta_0^K(t) h_K^{-d/2}\omega_K(t) \int_{\mathscr{U}_K^h} \left(\frac{2\mathscr{N}(t)}{\sqrt{Qu(t)}} + \mathscr{N}(t)^2 \right)$$

$$\leq 2 \left(\sum_{K\in\mathscr{T}_h} \eta_0^K(t)^2 h_K^{-d} \omega_K(t)^2 \left|\mathscr{U}_K^h\right| \sup_{\mathscr{U}_K^h} \frac{1}{Qu(t)} \right)^{1/2} \left(\sum_{K\in\mathscr{T}_h} \int_{\mathscr{U}_K^h} \mathscr{N}(t)^2 \right)^{1/2}$$

$$+ \max_{K\in\mathscr{T}_h} \left(\eta_0^K(t) h_K^{-d/2} \omega_K(t) \right) \left(\sum_{K\in\mathscr{T}_h} \int_{\mathscr{U}_K^h} \mathscr{N}(t)^2 \right)$$

The term with the time integral is treated in the same way and can be bounded by

$$\int_0^t \left[2 \left(\sum_{K\in\mathscr{T}_h} \eta_1^K(s)^2 h_K^{-d} \omega_K(s)^2 \left|\mathscr{U}_K^h\right| \sup_{\mathscr{U}_K^h} \frac{1}{Qu(s)} \right)^{1/2} \left(\sum_{K\in\mathscr{T}_h} \int_{\mathscr{U}_K^h} \mathscr{N}(s)^2 \right)^{1/2} \right.$$

$$\left. + \max_{K\in\mathscr{T}_h} \left(\eta_1^K(s) h_K^{-d/2} \omega_K(s) \right) \left(\sum_{K\in\mathscr{T}_h} \int_{\mathscr{U}_K^h} \mathscr{N}(s)^2 \right) \right] \mathrm{d}s.$$

Shape regularity implies that $\left|\mathscr{U}_K^h\right| \leq (\gamma^2/4) h_K^d$, for some γ depending only on the shape regularity σ_0. For the same reason there exists a number $M \in \mathbb{N}$, depending only on σ_0, that bounds the number of elements in each patch $\mathscr{U}_K^h$. It follows that

$$\int_0^t \langle \mathscr{R}(s) \,|\, \partial_t e(s) - I_h \partial_t e(s) \rangle \, \mathrm{d}s$$

$$\leq \gamma \left(\sum_{K\in\mathscr{T}_h} \alpha_K(0) \eta_0^K(0)^2 \right)^{1/2} A(0)^{1/2} + M \max \left(h_K^{-d/2} \omega_K(0) \eta_0^K(0) \right) A(0)$$

$$+ \gamma \left(\sum_{K\in\mathscr{T}_h} \alpha_K(t) \eta_0^K(t)^2 \right)^{1/2} A(t)^{1/2} + M \max_{K\in\mathscr{T}_h} \left(h_K^{-d/2} \omega_K(t) \eta_0^K(t) \right) A(t)$$

$$+ \gamma \int_0^t \left(\sum_{K\in\mathscr{T}_h} \alpha_K(s) \eta_1^K(s)^2 \right)^{1/2} A(s)^{1/2} \, \mathrm{d}s + M \int_0^t \max_{K\in\mathscr{T}_h} \left(h_K^{-d/2} \omega_K(s) \eta_1^K(s) \right) A(s) \, \mathrm{d}s.$$

Using Definition 3.5.3, and combining this with (3.30) we obtain (3.47) which proves the lemma. □

3.6 Main results

For (3.47) to be useful we must control the terms containing $A(t)$ on the right-hand side with those left hand side. There are two main ways of doing this. The first way gives rise to conditional estimates.

3.6.1 Theorem (Conditional aposteriori estimate)**.** *Let u be the solution of Problem 2.1.3 and u_h the finite element solution of Problem* (2.5.3)*. Assume that, for $t \in [0,T]$, the following condition holds*

$$\mathscr{E}^*_{\infty,0}(t) + \mathscr{E}_{\infty,1}(t) \leq \frac{1}{8} \tag{3.52}$$

where

$$\mathscr{E}^*_{\infty,0}(t) := \sup_{s\in[0,t]} \mathscr{E}_{\infty,0}(s). \tag{3.53}$$

Then there exists a constant $C = C[u_h, t]$ such that the following aposteriori estimate holds

$$\int_0^t \int_\Omega (Vu_h - Vu)^2 Qu + \frac{1}{2} \sup_{[0,t]} \int_\Omega |Nu_h - Nu|^2 Qu \leq C\left(\mathscr{E}_0^2 + \mathscr{E}^2(t)\right) \tag{3.54}$$

where

$$\mathscr{E}(t)^2 := 8\left(\mathscr{E}^*_{2,0}(t)^2 + \mathscr{E}_{2,1}(t)^2\right), \tag{3.55}$$

$$\mathscr{E}^*_{2,0}(t) := \sup_{[0,t]} \mathscr{E}_{2,0}. \tag{3.56}$$

Furthermore, the constant $C = C[u_h, t]$ is bounded by

$$\exp \int_0^t 4\varrho(s)\,\mathrm{d}s = \exp \int_0^t \left(2\left\|\partial_t u_h(s)\right\|^2_{\mathrm{L}_\infty(\Omega)} + 4\left\|\nabla \partial_t u_h(s)\right\|_{\mathrm{L}_\infty(\Omega)}\right) \mathrm{d}s. \tag{3.57}$$

.

Proof The theorem is derived from (3.47). Introduce $A^*(t) := \sup_{[0,t]} A$, apply Hölder inequality, and Young inequality with parameter $\mu = 1/8$ to obtain

$$\begin{aligned} A(t) + B(t) \leq & \mathscr{E}_0^2 + \mu A(t) + \frac{1}{\mu}\mathscr{E}_{2,0}(t)^2 + \mu A^*(t) + \frac{1}{\mu}\mathscr{E}_{2,1}(t)^2 \\ & + 2\mathscr{E}_{\infty,0}(t)A(t) + 2A^*(t)\mathscr{E}_{\infty,1}(t) \\ & + 2\int_0^t \varrho(s)A(s)\,\mathrm{d}s. \end{aligned}$$

Taking the supremum over $[0,t]$ on both sides, recalling that B is nondecreasing, and collecting terms we obtain

$$\begin{aligned} A^*(t) + B(t) \leq & \mathscr{E}_0^2 + \frac{1}{4}A^*(t) + 8\left(\mathscr{E}_{2,0}^*(t)^2 + \mathscr{E}_{2,1}(t)^2\right) \\ & + 2\left(\mathscr{E}_{\infty,0}^*(t) + \mathscr{E}_{\infty,1}(t)\right)A^*(t) + 2\int_0^t \varrho(s)A^*(s)\,\mathrm{d}s. \end{aligned}$$

Exploiting (3.52) we reach

$$\frac{1}{2}A^*(t) + B(t) \leq \mathscr{E}_0^2 + 8\left(\mathscr{E}_{2,0}^*(t)^2 + \mathscr{E}_{2,1}(t)^2\right) + 2\int_0^t \varrho(s)A^*(s)\,\mathrm{d}s, \tag{3.58}$$

which enables us to apply Gronwall inequality A.2.1 and conclude (3.54) and (3.57). □

In the light on the stability result of Lemma 2.4.1 we can relax assumption (3.52) at the cost of living with a looser upper bound. This is the second way to get an estimate.

3.6.2 Theorem (Unconditional aposteriori estimate)**.** *Suppose the assumptions of Theorem 2.4.1 are verified. Then there exist $C = C[u_h, f, t]$ and $C' = C'[f, g, t]$ such that*

$$\begin{aligned} \int_0^t \int_\Omega (Vu_h - Vu)^2 Qu + \frac{1}{2}\int_\Omega \sup_{[0,t]} \int_\Omega |Nu_h - Nu|^2\, Qu \\ \leq C\left(\mathscr{E}_0^2 + \mathscr{E}_2(t)^2 + C'\mathscr{E}_\infty(t)\right) \end{aligned} \tag{3.59}$$

where

$$\mathscr{E}_2(t)^2 := 4(\mathscr{E}^*_{2,0}(t)^2 + \mathscr{E}_{2,1}(t)^2),$$

$$\mathscr{E}_\infty(t) := 4(\mathscr{E}_{\infty,0}(t) + \mathscr{E}_{\infty,1}(t)),$$

and the constants are bounded by

$$C[u_h, f, t] \leq \exp \int_0^t \left(2 \left\| \partial_t u_h(s) \right\|^2_{\mathrm{L}_\infty(\Omega)} + 4 \left\| \nabla \partial_t u_h(s) \right\|_{\mathrm{L}_\infty(\Omega)} + \left\| f(s) \right\|_{\mathrm{L}_\infty(\Omega)^2} \right) \mathrm{d}s,$$

$$C'[f, g, t] \leq \int_\Omega Qg(0) + \left\| \partial_t g \right\|_{\mathrm{L}_1(\partial\Omega \times (0,t))}.$$

Proof The proof is a direct combination of Lemma 3.5.4, the elementary fact that

$$\int_\Omega \left| Nu_h(t) - Nu(t) \right|^2 Qu(t) \leq 4 \int_\Omega Qu(t), \tag{3.60}$$

and the stability Theorem 2.4.1 which gives a bound for the last integral. □

3.6.3 Remark (About the conditional estimate)**.** Theorem 3.6.1 is a conditional result. Such results are typical in nonlinear analysis. The condition can be interpreted as the approximate solution u_h having to be "close enough" to the exact solution u for the estimate to hold and is the result of linearizing the equation about u (or u_h). What is important to notice in our estimate is that *the condition can be automatically checked by a computer* since all the quantities that enter in it are *aposteriori quantities* (one can think of us having linearized about u_h, a known quantity, in some indirect way, making the constants depend on computable quantities). This is in contrast with most results on aposteriori analysis for nonlinear problems [Ver98] where conditions *that cannot be automatically checked are assumed*.

3.7 The treatment of boundary data

As promised earlier in this chapter we now remove Hypothesis 3.3.2, so we allow for

$$\partial_t(u_h - u)|_{\partial\Omega} = \partial_t(g_h - g) \neq 0. \tag{3.61}$$

We will derive an estimate including the boundary value approximation assuming that

$$g_h = I_h g, \tag{3.62}$$

where I_h continues to denote the Scott-Zhang interpolator. We think that this result can be extended to some more practical interpolators, like the Lagrange interpolator; however we did not pursue this issue as the analysis becomes technically complicated and far from clear.

We start by decomposing the error $e = u_h - u$ in two parts

$$e = e_0 + \epsilon, \tag{3.63}$$

where

$$e_0 := u_h - \tilde{g}_h - u + \tilde{g}, \tag{3.64}$$

$$\epsilon := \tilde{g}_h - \tilde{g}. \tag{3.65}$$

Here $\tilde{g}_h$ and $\tilde{g}$ denote extensions of g_h and g to the whole domain Ω (cf. [SZ90, (5.5)]).

The main difficulty is that the error equation (3.12) is no longer valid for $\phi = \partial_t e$ and $\phi_h = I_h \partial_t e$ as the function $\partial_t e$ is not admissible, for failing to vanish at the boundary.

Notice however that nothing prevents the extension of the residual functional $\mathscr{R}$ to all of $\mathrm{W}_1^1(\Omega)$. (It was defined in (3.11) as acting on $\mathring{\mathrm{W}}_1^1$.) This means that we can take $\phi = \partial_t e$ in (3.12) and obtain

$$\begin{aligned} \langle \mathscr{R} \,|\, \partial_t e \rangle &= \langle \mathscr{R} \,|\, \partial_t e_0 \rangle + \langle \mathscr{R} \,|\, \partial_t \epsilon \rangle \\ &= \langle \mathscr{R} \,|\, \partial_t e_0 - I_h \partial_t e_0 \rangle + \langle \mathscr{R} \,|\, \partial_t \epsilon \rangle \,. \end{aligned} \tag{3.66}$$

The Galerkin orthogonality can be applied directly to the part containing the admissible error (by "admissible" we mean $\in \mathring{\mathrm{W}}_1^1$). In particular, we can derive the residual representation for the first term

$$\langle \mathscr{R} \,|\, \partial_t (e_0 - I_h e_0) \rangle = \langle r, \partial_t (e_0 - I_h e_0) \rangle + \langle j, \partial_t (e_0 - I_h e_0) \rangle_{\Sigma_h} \,. \tag{3.67}$$

Some orthogonality can still be exploited to treat the last term in (3.66). Namely, using the properties of the Scott-Zhang interpolator I_h we observe that

$$\begin{aligned} I_h \epsilon|_{\partial\Omega} &= (I_h \tilde{g}_h)|_{\partial\Omega} - (I_h g)|_{\partial\Omega} \\ &= I_h \left(\tilde{g}_h|_{\partial\Omega} \right) - I_h \left(\tilde{g}|_{\partial\Omega} \right) \\ &= I_h I_h g - I_h g \\ &= 0. \end{aligned}$$

Notice that the invariance of $\mathring{\mathbb{V}}_h^\ell$ under I_h as a transformation is crucial for this argument to go through.

This implies in particular that $\partial_t I_h \epsilon \in \mathring{\mathbb{V}}_h^\ell$, from which we infer

$$\langle \mathscr{R} \,|\, \partial_t I_h \epsilon \rangle = 0. \tag{3.68}$$

Now the residual representation can be derived, by integrating by parts in space as usual, as follows

$$\langle \mathscr{R} \,|\, \partial_t \epsilon \rangle = \langle \mathscr{R} \,|\, \partial_t (\epsilon - I_h \epsilon) \rangle$$

$$= \langle r, \partial_t(\epsilon - I_h\epsilon)\rangle + \langle j, \partial_t(\epsilon - I_h\epsilon)\rangle_{\Sigma_h} + \langle \beta - \beta_h, \partial_t\epsilon\rangle_{\partial\Omega}$$

where $\beta := (\nabla u \cdot \boldsymbol{\nu})/Qu$ and $\beta = (\nabla u_h \cdot \boldsymbol{\nu})/Qu_h$.

We thus end up with the following equation

$$\langle \mathscr{R} \,|\, \partial_t e\rangle = \langle r, \partial_t e - I_h\partial_t e\rangle + \langle j, \partial_t e - I_h\partial_t e\rangle + \langle \beta - \beta_h, \partial_t\epsilon\rangle_{\partial\Omega}\,. \tag{3.69}$$

In order to obtain a lower bound of the left-hand side of the error equation, we proceed in the same fashion as in Section 3.4 and thereby we derive again (3.30).

The first term on the right-hand side is also treated as in Section 3.5 (owing to the fact that the Scott-Zhang interpolator can be taken all the way up to the boundary).

We thus need only to bound the integral in time of the last term. To this end we exploit the fact that I_h preserves boundary values and the fact that $\beta, \beta_h \leq 1$ to reach

$$\langle \beta - \beta_h, \partial_t\epsilon\rangle_{\partial\Omega} \leq \|\partial_t\epsilon\|_{\mathrm{L}_1(\partial\Omega)} = \|\partial_t g - I_h\partial_t g\|_{\mathrm{L}_1(\partial\Omega)} =: \dot{\mathscr{E}}_{\partial\Omega}.$$

Once $I_h g$ is at hand, the norm on the right-hand side is a computable quantity.

We then have the following generalization of Lemma (3.5.4)

3.7.1 Lemma (Residual estimate with boundary values)**.** *The following inequality holds for each $t \in [0, T]$:*

$$\begin{aligned} A(t) + B(t) \leq{}& \mathscr{E}_0^2 + \mathscr{E}_{\partial\Omega}(t) \\ &+ 2\mathscr{E}_{2,0}(t)A(t)^{1/2} + 2\mathscr{E}_{\infty,0}A(t) \\ &+ 2\int_0^t \dot{\mathscr{E}}_{2,1}(s)A(s)^{1/2}\,\mathrm{d}s + 2\int_0^t \dot{\mathscr{E}}_{\infty,1}(s)A(s)\,\mathrm{d}s \end{aligned}$$

$$+ 2 \int_0^t \varrho(s) A(s) \, \mathrm{d}s.$$

where

$$\mathscr{E}_{\partial\Omega}(t) = \int_0^t \dot{\mathscr{E}}_{\partial\Omega}. \tag{3.70}$$

We can then obtain extended versions of Theorems 3.6.1 and 3.6.2 by just adding $\mathscr{E}_{\partial\Omega}$ to the estimators of these theorems.

Chapter 4

Numerical experiments: reliability tests

In this chapter we present the computational results that have been obtained in order to test the reliability of the upper bound derived in chapter 3.

We begin by describing briefly the implementation of the finite element method and the semi-implicit time stepping method, which linearizes the equation and allows to use linear solvers at each time step in a stable way.

We then proceed to exhibit numerical results regarding the exact error and the corresponding error estimators for examples where the exact solution is known.

Finally we show some results that have been obtained for problems without an explicit solution.

4.1 Implementation

Space-time discretization of the mean curvature flow

We introduce first the numerical scheme for the time stepping and combine it with the spatial finite element method to obtain a fully discrete scheme. This is the basis of a computer implementation of the Cauchy-Dirichlet Problem 2.1.3.

In order to implement a numerical scheme to approximate solutions of problem 2.1.3, Problem 2.5.3 needs to be further discretized in time. Following ideas by Deckelnick & Dziuk [DD00, Dzi99] we introduce a *semi-implicit time stepping scheme* associated to Problem 2.1.3 as follows.

4.1.1 Definition (Time-discrete semi-implicit scheme)**.** Given $N \in \mathbb{Z}^+$ and a finite set of *times* (or *instants*) $\{t_n : n = 0, \dots, N\}$ such that $0 = t_0 < t_1 < \dots < t_N = T$ and, for all $n \in [1 : N]$, denote by $\tau_n := t_n - t_{n-1}$ the *stepsize* at the n-th timestep (t_{n-1}, t_n). Given $U^0 = g(x, 0)$, for each $n \in [1 : N]$, solve the following

4.1.2 Problem. *Find $U^n \in \mathrm{C}^2(\Omega) \cap \mathrm{C}(\overline{\Omega})$ such that*

$$\frac{U^n - U^{n-1}}{\tau_n Q U^{n-1}} - \operatorname{div} \frac{\nabla U^n}{Q U^{n-1}} = f^n, \text{ in } \Omega; \tag{4.1}$$

$$U^n = g^n, \text{ on } \partial\Omega; \tag{4.2}$$

Notice that equation 4.1 is a linear elliptic equation which can implemented rather easily. We discretize it in space by using a finite element approach which parallels that in section 2.5. Namely, we consider the following scheme.

4.1.3 Problem. *Given $g_h(0) \in \mathbb{V}_h^\ell$ (an interpolant of $g(0)$), and $\tilde{g}_h^n$ (an interpolant of $g(t_n)$), we look for a sequence of functions $U_h^n \in \mathbb{V}_h^\ell$ recursively defined by*

$$\left\langle \frac{\nabla U^n}{Q U^{n-1}}, \nabla \phi_h \right\rangle + \left\langle \frac{U^n}{\tau_n Q U^{n-1}}, \phi_h \right\rangle = \left\langle \frac{U^{n-1}}{\tau_n Q U^{n-1}} + f^n, \phi_h \right\rangle, \ \forall \phi_h \in \mathring{\mathbb{V}}_h^\ell; \tag{4.3}$$

$$U_h^n - \tilde{g}_h^n \in \mathring{\mathbb{V}}_h^\ell. \tag{4.4}$$

This scheme is unconditionally stable [DD00, Proposition 2.1]. It has been shown also to converge with order $\mathrm{O}(\tau + h)$, where $\tau = \max \tau_n$, under the hy-

pothesis that $\tau \leq \delta_0 h$ for some $\delta_0 > 0$ and that u satisfies some rather strong regularity properties [DD00, Proposition 3.3].

All our results are based on this scheme. The implementation uses the C finite element toolbox ALBERT, kindly provided by Kunibert Siebert & Alfred Schmidt [SS00].

We will assume no stronger regularity than needed for the estimators to make sense in our examples. Actually we will be analyzing some singular situations, and show relations between singular behavior of the solution and that of the estimators. This is not covered by Deckelnick & Dziuk in their work on apriori estimates [DD00].

Unless otherwise mentioned all our computations are based on *piecewise linear finite elements*, commonly known also as $\mathbb{P}^1$-elements.

Practical version of the error estimators

In the reliability tests, we have to compute a discrete version of the global estimators introduced in Definition 3.5.3, which are in turn computed using the local indicators 3.5.2. A close look at the indicators

$$\eta_i^K(t) := h_K^{d/2}(C_1 \left\|(\partial_t)^i r(t)\right\|_{\mathrm{L}_d(K)} + C_2 \left\|(\partial_t)^i j(t)\right\|_{\mathrm{L}_\infty(\partial K)}) \tag{4.5}$$

for $i = 0, 1$, shows an L_∞ norm which might prove to be hard to compute in principle. However, for piecewise linear elements, the jump is itself a constant function (being the gradient constant on each side and the denominator Qu_h consequently constant), this norm can be replaced, using the following $(\mathrm{L}_\infty, \mathrm{L}_2)$ inverse estimate

$$\|v\|_{\mathrm{L}_\infty(\partial K)} \leq C h^{(1-d)/2} \|v\|_{\mathrm{L}_2(\partial K)} \tag{4.6}$$

obtained by equivalence of norms on finite dimensional spaces and scaling. This legitimizes the use of the more practical indicators

$$\eta_i^K(t) := h_K^{d/2} C_1 \left\| (\partial_t)^i r(t) \right\|_{\mathrm{L}_d(K)} + h_K^{1/2} C_2 \left\| (\partial_t)^i j(t) \right\|_{\mathrm{L}_2(\partial K)}. \tag{4.7}$$

The initial error can be computed exactly, modulo quadrature and round-off errors of course. We will be concerned with the bulk part of the estimator, that is $\mathscr{E}$ defined in (3.55).

4.2 Problems with known exact solution

We now present the numerical results obtained for certain problems where the exact solution is known. These tests are important as they we can tell to what extent our estimators are reliable by comparing the estimators to the exact error, which is computable in this case. In what follows, in addition to the notation introduced earlier, will make use of

$$E(t) = E[u, u_h](t) = \left(\int_0^t \int_\Omega |Vu_h - Vu| \, Qu + \sup_{[0,t]} |Nu_h - Nu| \, Qu \right), \tag{4.8}$$

$$\widehat{\mathscr{E}}(t) = \mathscr{E}_0 + \sup_{[0,t]} \mathscr{E}_{2,0} + \mathscr{E}_{2,1} \tag{4.9}$$

$$\mathscr{E}_\infty = \sup_{[0,t]} \mathscr{E}_{\infty,0} + \mathscr{E}_{\infty,1}. \tag{4.10}$$

where the notation is introduced in Definition 3.5.3.

All the integrals above are to be understood as quadratures. While we use ALBERT's built in Gaussian quadrature in space, we use a simple midpoint rule for the integrals in time and the sup in time is replaced by a max over the time nodes.

A problem with exact boundary and initial approximation

We start with a simple case:

4.2.1 Example (Exact solution on a square)**.** Let

$$u(x,y;t) = t\left(\sin(t) - \sin(t - x(1-x)y(1-y))\right) \tag{4.11}$$

for $(x,y) \in \Omega \times (0,T) := (0,1) \times (0,1) \times (0,8)$. Then $u \in \mathrm{C}^\infty(\overline{\Omega})$, its initial and boundary values are zero. Thus the initial and boundary interpolation do not have any effect on our computations as they are solved exactly. (The right hand side f can be derived from u, by using the equation.)

We perform a series of computations, on uniform meshes, with the following meshsizes

$$h \in \{0.5000, 0.2500, 0.1250, 0.0625, 0.0312, 0.0156\}.$$

We report all the results in form of graphs where the abscissa is the time variable, so we can track the behavior of the errors and estimates in time. The first series of graphs 4.1 shows the behavior of the exact spatial errors against time in the geometric quantities and the more customary Sobolev norms for the heat equation.

It is worth comparing this to the similar graph where the errors are replaced by estimators 4.3.

To understand the asymptotic behavior from the numerical point of view, we calculate and plot the *experimental order of convergence* of the error $\widehat{\mathscr{E}}(t_n)$ at each time t_n.

The EOC of a sequence of a given quantity e_i — which could be the error or the estimator — that depends on the refinement level i with h_i as meshsize is

given by

$$\frac{\log(e_{i+1}/e_i)}{\log(h_{i+1}/h_i)}.$$

As shown by Figure 4.2, the geometric error EOC 1 as expected from the theory. Although the terms involving the normal velocity tend to decrease faster (not shown here), it is the the sum of the two terms that is of order 1.

A crucial test for the estimators is whether their asymptotic behavior matches that of the error. That is we need to compare the two EOC. In figure 4.3 we show the behavior of the proper estimator $\widehat{\mathscr{E}}$ and the conditional estimator.

It is crucial for reliability, that the order of convergence for the error and the estimator match. It can be seen from the graphics that this match is realized in the long run. Indeed, in Figure 4.4 we plot the ratio $E(t)/\widehat{\mathscr{E}}(t)$. This ratio converges to a function of time. This function represents the constant in front of the estimator, that is bounded by the exponential constant. In this case, this function is decreasing and we do not detect any exponential behavior.

A fact which is worth noticing is that the order of convergence of the conditional estimators, seems to performs slightly worse than 1: there is a clear numerical indication that it is closer to 0.95. The discrete norm — we take the liberty to abuse this term — in which the conditional estimators are computed in space are stronger than those for the proper estimators — by proper we mean the elliptic and parabolic estimators introduced in 3.5.3. This is a reason why we can expect worse behavior. The oscillatory nature of the solution is also responsible for accentuating the discrepancy between the proper and conditional estimators.

Problem with curved boundary

Although in our analysis we did not include curved boundaries, it happens very frequently that this is not a major problem. The following example is very similar to Example 4.2.1, albeit the problem is considered on the disk $\mathrm{B}_1(0)$. This example was used by Gerhard Dziuk [Dzi99] for numerical tests and we shall refer to it as *the Dziuk benchmark*.

4.2.2 Example (Dziuk benchmark: exact solution on a disk)**.** Let

$$u(x, y; t) = -\sin(1 - t) - \sin(t - x^2 - y^2) \tag{4.12}$$

for $(x, y) \in \Omega \times (0, T) := \mathrm{B}_1(0) \times (0, 10)$. Then $u \in \mathrm{C}^\infty(\overline{\Omega})$. Notice that in contrast to the situation in Example 4.2.1 that the boundary interpolation cannot be exact in this case, because the boundary is curved. Notice that the boundary value is homogeneous though. The initial solution is non zero and needs to be interpolated carefully to obtain satisfactory results. As we shall see in Example 4.3.1, it's important to take the minimal surface projection to an associated problem as discrete initial value. Otherwise, the data will not have any noticeable effect on our computations as they are solved exactly. (The right hand side f can be derived from u, by using the equation.)

The meshsizes of the quasi-uniform triangulations that we compute the solution for are

$$h \in \{0.7368, 0.4203, 0.2219, 0.1137, 0.0575\}. \tag{4.13}$$

We output the same kind of data as for Example 4.2.1: in Figures 4.5 and 4.7 we have the error and their estimators respectively, while in Figure 4.6 we see the EOC of the error.

Also in this example we can see that the estimators have the expected asymptotic behavior numerically.

Due to the matching asymptotic behavior the ratio between the error and the estimators converges (as a function of time) to a function of time. In this case, this function is decreasing and we do not detect any exponential behavior either as shown in figure 4.8. The nature of the problem is very similar to the one in Example 4.2.1. Notice that we did not take into account the boundary approximation in the computation of the error. The disk having a well-behaved boundary, this does not seem to give any problem on that side.

Shrinking sphere

We take the shrinking sphere of Example 2.2.7 as a benchmark for one more test. Here we will have a blow up at the boundary for $t = 0.5$. The meshsizes are given by the sequence

$$h \in \{1.0000, 0.5000, 0.2500, 0.1250, 0.0625, 0.0312, 0.0156, 0.0078\}. \tag{4.14}$$

As before we report the error in Figure 4.9 and its asymptotic behavior in Figure 4.10. This is done also for the estimators in Figure 4.11. In Figure 4.12 we report the ratio between the error and the estimator. In this case the ratio increases as the time increases. It's interesting to see that the ratio actually blows up as $t \to 0.5$. This might be an indication of the exponential behavior.

4.3 The initial condition

In our computations, whenever possible we take the minimal surface projection as an interpolation for the initial values. The minimal surface projection of a given function v is defined as the finite element solution v_h of the elliptic boundary value problem:

$$\left\langle \frac{\nabla v_h}{Q u_h}, \phi_h \right\rangle = \left\langle \frac{\nabla v}{Q v}, \phi_h \right\rangle. \tag{4.15}$$

It is a "projection" with respect to the surface area energy.

To show how important this choice is we reconsider the example of the shrinking sphere.

4.3.1 Example (Initial condition approximation)**.** We solve again the shrinking sphere problem. This time we take as discrete initial value the interpolant of the initial value. We plot the results on the same graph of those obtained for the solution with the minimal projection. Notice the poor initial approximation of the error (Figure 4.13) and the estimators (Figure 4.14).

4.4 Example without exact solution

As a last series of examples we will consider the situation where the domain is non-convex and the exact solution might cease to exist.

4.4.1 Example. This is given by the catenoid described in Example 1.2.3. The critical height is $H^* = \log(2+\sqrt{3})/2 \approx 0.6585$. We will take three different situations where $H = 0.50, 0.60, 0.70$.

The behavior of these estimators is given and discussed in Figure 4.15.

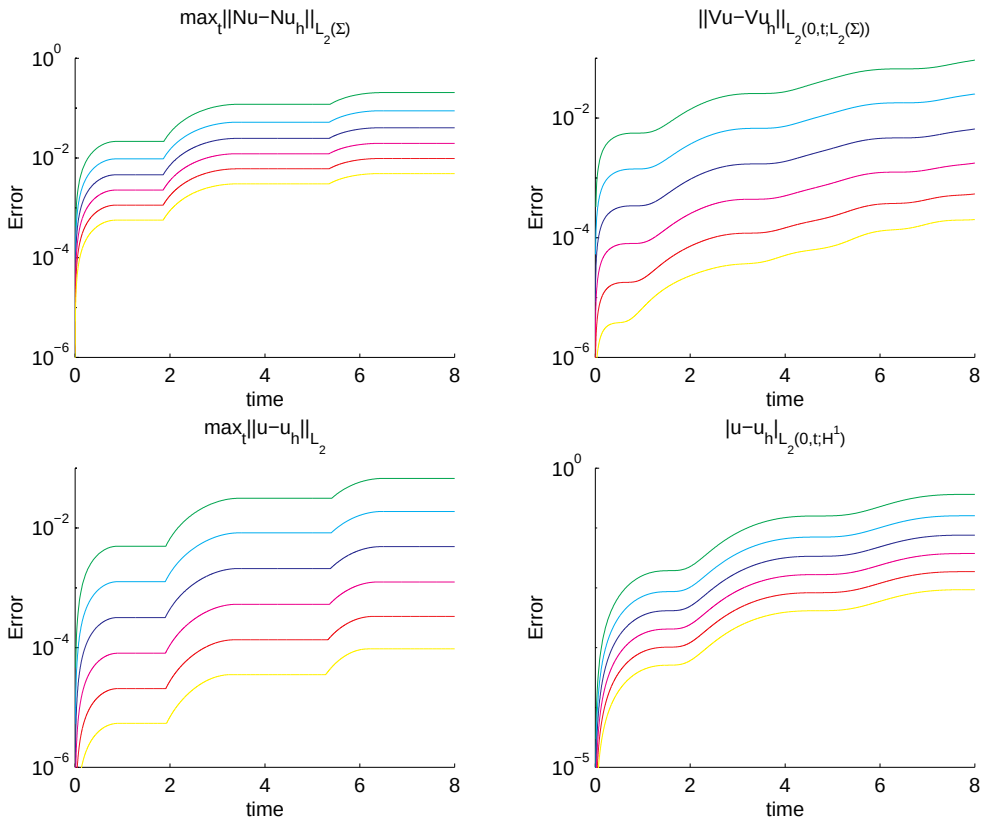

Figure 4.1: We report the error, between u_h and u in Example 4.2.1, measured with the geometric quantities and the more customary Sobolev norms used for the heat equation. The different colors stand for the different mesh-sizes $h \in \{0.5000, 0.2500, 0.1250, 0.0625, 0.0312, 0.0156\}$. It's worth noticing the similar behavior that norms and geometric quantities have, which justifies the use of geometric quantities as an error concept.

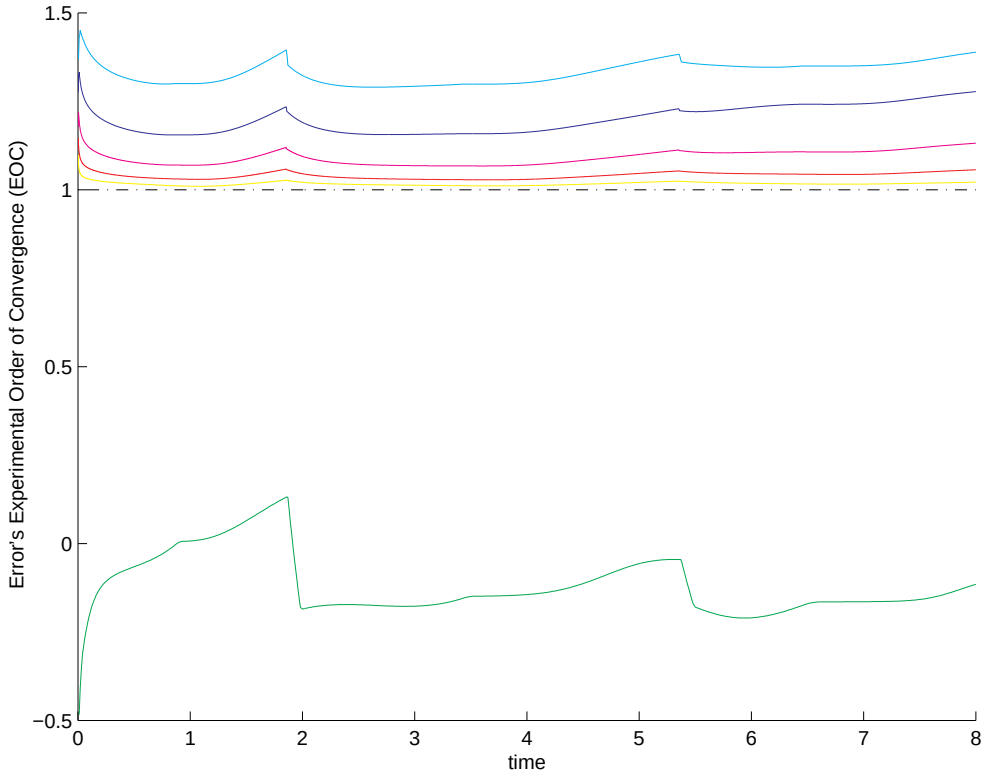

Figure 4.2: The experimental order of convergence of the geometric error E gets close to 1 as the meshsize decreases, in Example 4.2.1. The different colors stand for the different meshsizes $h = \{0.5000, 0.2500, 0.1250, 0.0625, 0.0312, 0.0156\}$. This is the rate that is expected in theory. The terms involving the normal velocity tend to converge faster (not shown here), but since we have only one estimate for both quantities we must look at the sum.

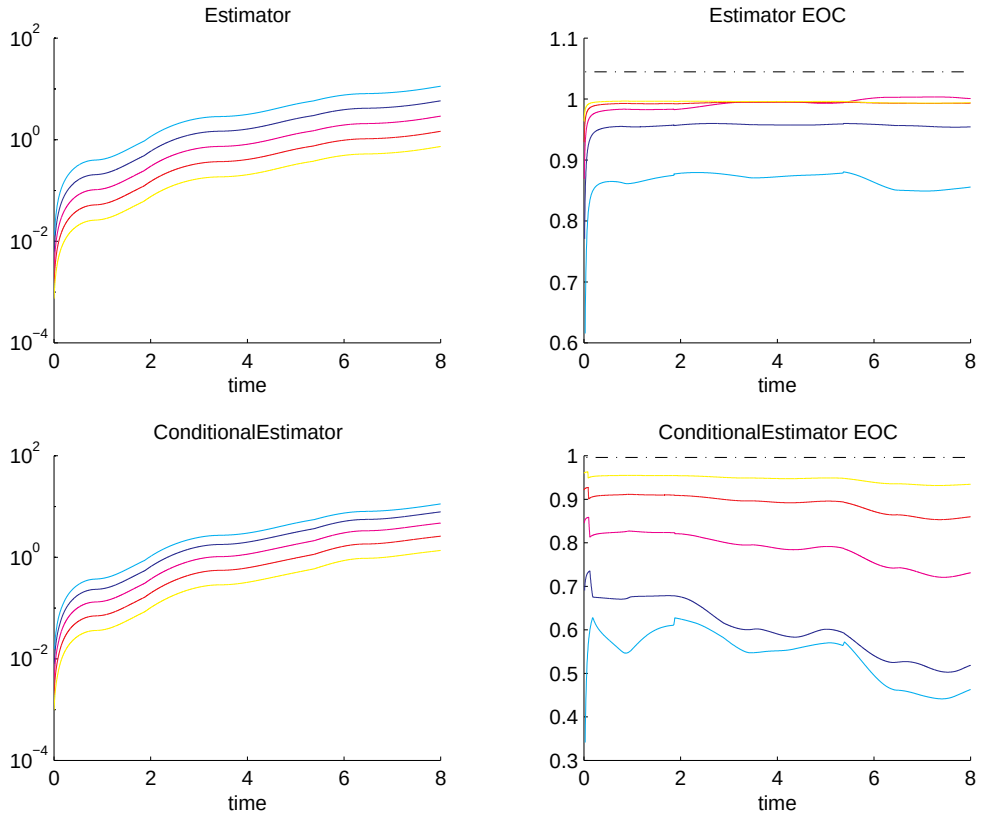

Figure 4.3: In these plots we exhibit on the left-hand side both the proper estimator $\widehat{\mathscr{E}}$ and the conditional estimator $\mathscr{E}_\infty$ relative to Example 4.2.1. The different colors stand for the different meshsizes $h \in \{0.5000, 0.2500, 0.1250, 0.0625, 0.0312, 0.0156\}$. Their EOC is computed and plotted on the right hand side. It's fundamental for the EOC of $\widehat{\mathscr{E}}$ to get close to 1 as the meshsize decreases. It is interesting to see that the conditional estimator converges at a slower rate, meaning that the unconditional estimate in Theorem 3.6.2 is improved by the conditional estimate Theorem 3.6.1 once the approximate solution is close enough to the exact one.

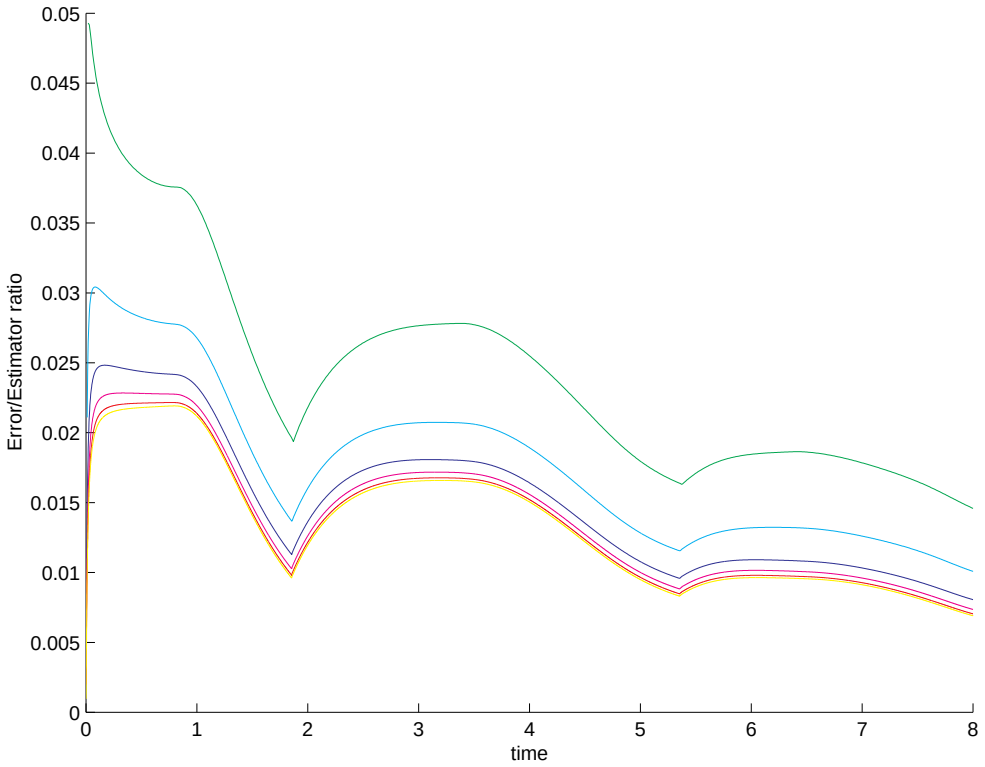

Figure 4.4: This plot represents the ratio between the exact error E and the estimator $\widehat{\mathscr{E}}$ for Example 4.2.1. This is a crucial test for the estimators, the fact that the ratio converges as $h \to 0$ to a function of time means that the asymptotic behavior of the error and the estimator are the same. The different colors stand for the different meshsizes $h \in \{0.5000, 0.2500, 0.1250, 0.0625, 0.0312, 0.0156\}$. The theory derived in Chapter 3 gives a worst case scenario prediction of a ratio that is an increasing exponential. In this case, we don't detect this behavior.

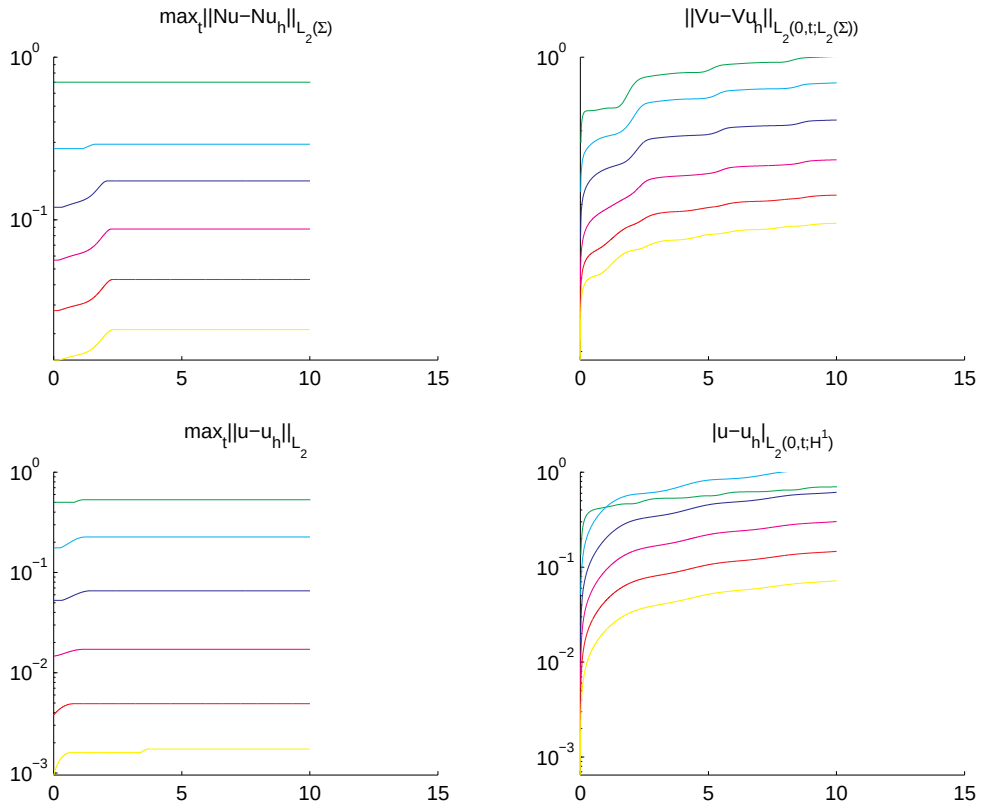

Figure 4.5: We report the error measured with the geometric quantities and the more customary Sobolev norms used for the heat equation. Different colors stand for different meshsizes $h \in \{0.7368, 0.4203, 0.2219, 0.1137, 0.0575\}$ and the abscissa is the time variable. It's worth noticing the similar behavior, which justifies the use of geometric quantities as an error concept.

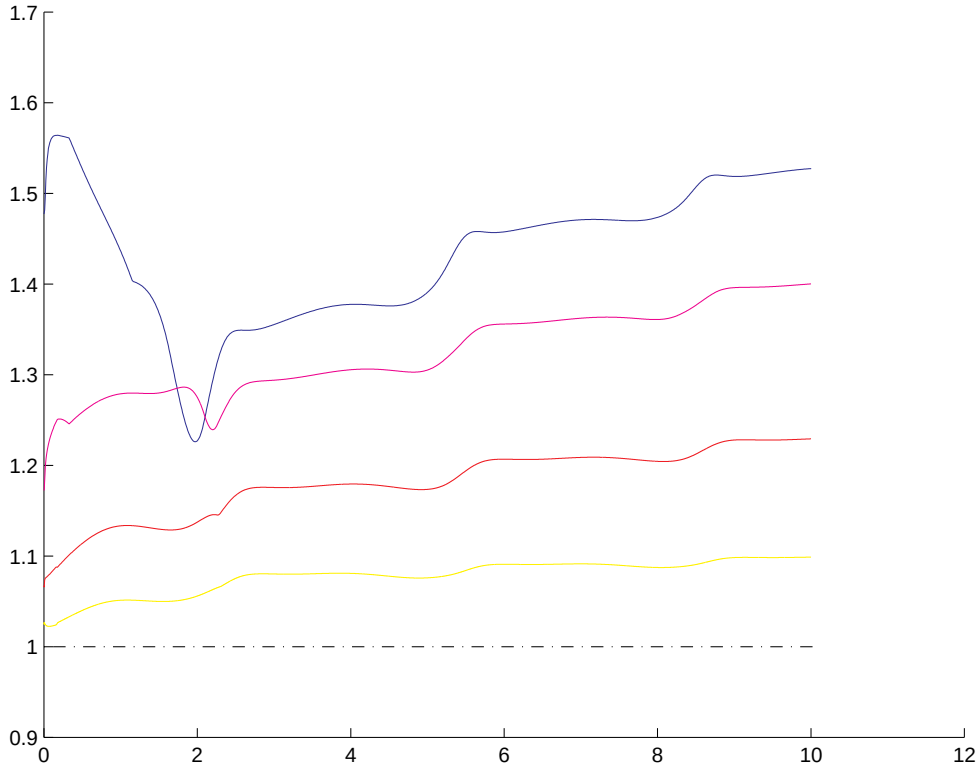

Figure 4.6: The EOC of the geometric error E gets close to 1 as the meshsize decreases. This is the rate that is expected in theory. In these plots the rate seems to be slightly better than 1 in a first stage. Different colors stand for different meshsizes $h \in \{0.7368, 0.4203, 0.2219, 0.1137, 0.0575\}$ and the abscissa is the time variable.

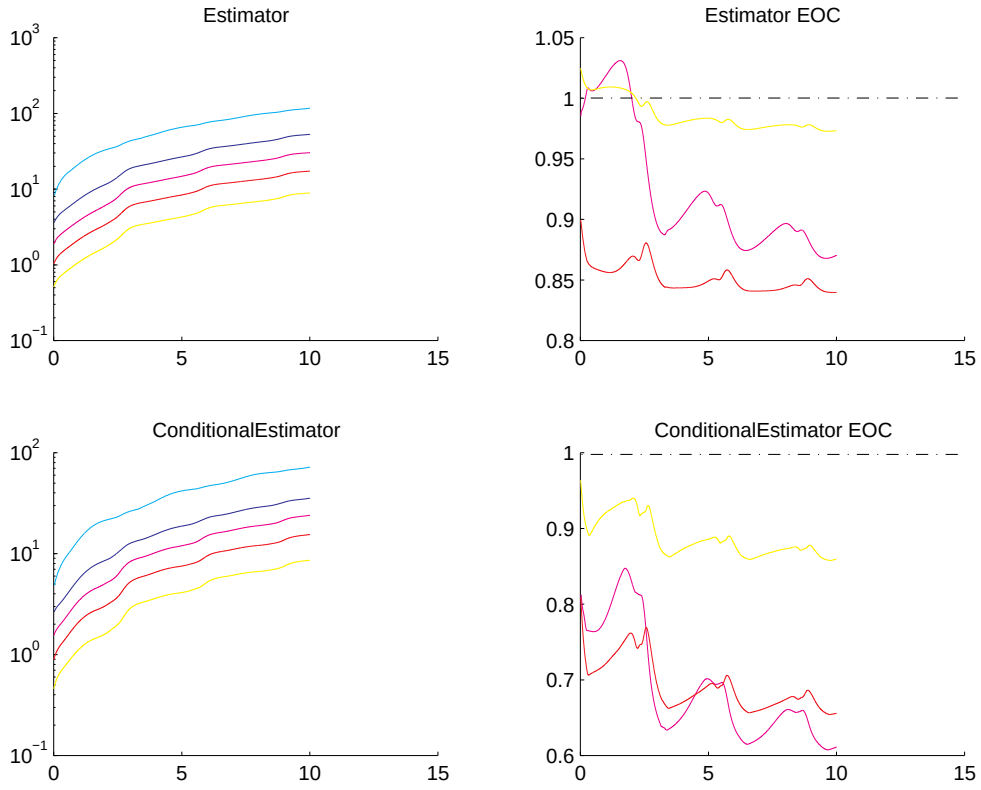

Figure 4.7: In these plots we exhibit on the left-hand side both the proper estimator $\widehat{\mathscr{E}}$ and the conditional estimator $\mathscr{E}_\infty$. Their EOC is computed and plotted on the right hand side. Different colors stand for different meshsizes $h \in \{0.7368, 0.4203, 0.2219, 0.1137, 0.0575\}$ and the abscissa is the time variable. As before we see that $\widehat{\mathscr{E}}$ converges with an asymptotic rate of 1. Again the discrepancy between the EOC for the proper and conditional estimators is striking. Notice that the conditional estimator doesn't need to be asymptotically zero. It has to be bounded by a small number though.

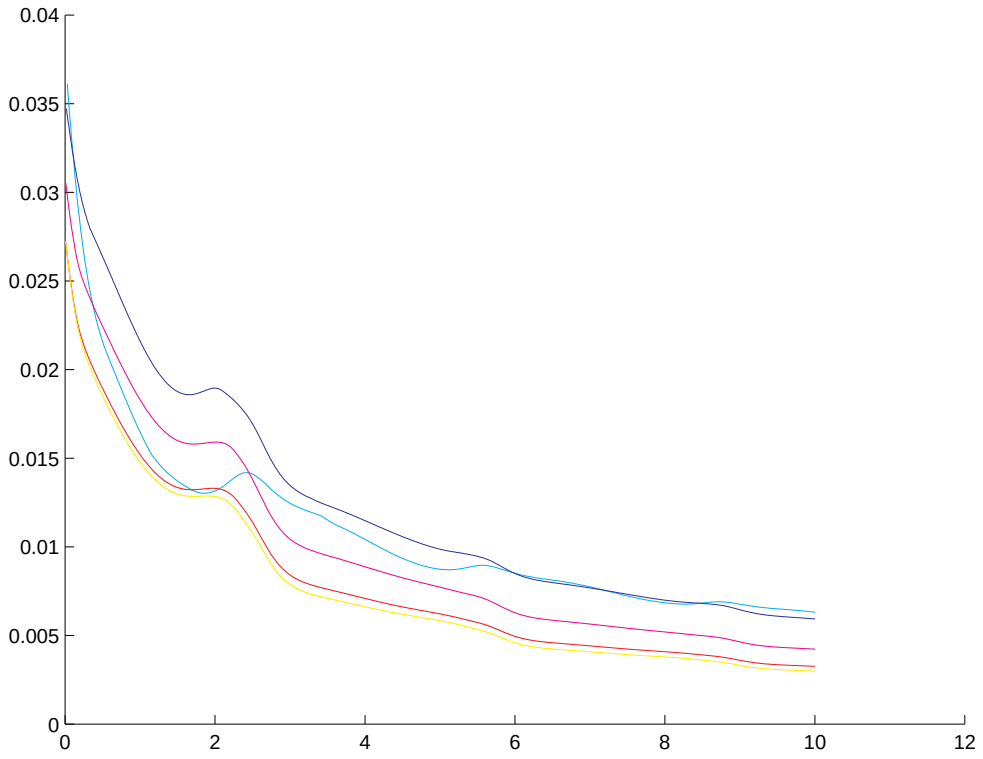

Figure 4.8: This plot represents the ratio between the exact error E and the estimator $\widehat{\mathscr{E}}$. This is a crucial test for the estimators, the fact that the ratio converges as $h \to 0$ to a function of time means that the asymptotic behavior of the error and the estimator are the same. Different colors stand for different meshsizes $h \in \{0.7368, 0.4203, 0.2219, 0.1137, 0.0575\}$ and the abscissa is the time variable. The theory derived in Chapter 3 gives a worst case scenario prediction of a ratio that is an increasing exponential. This is another case in which we don't detect this behavior.

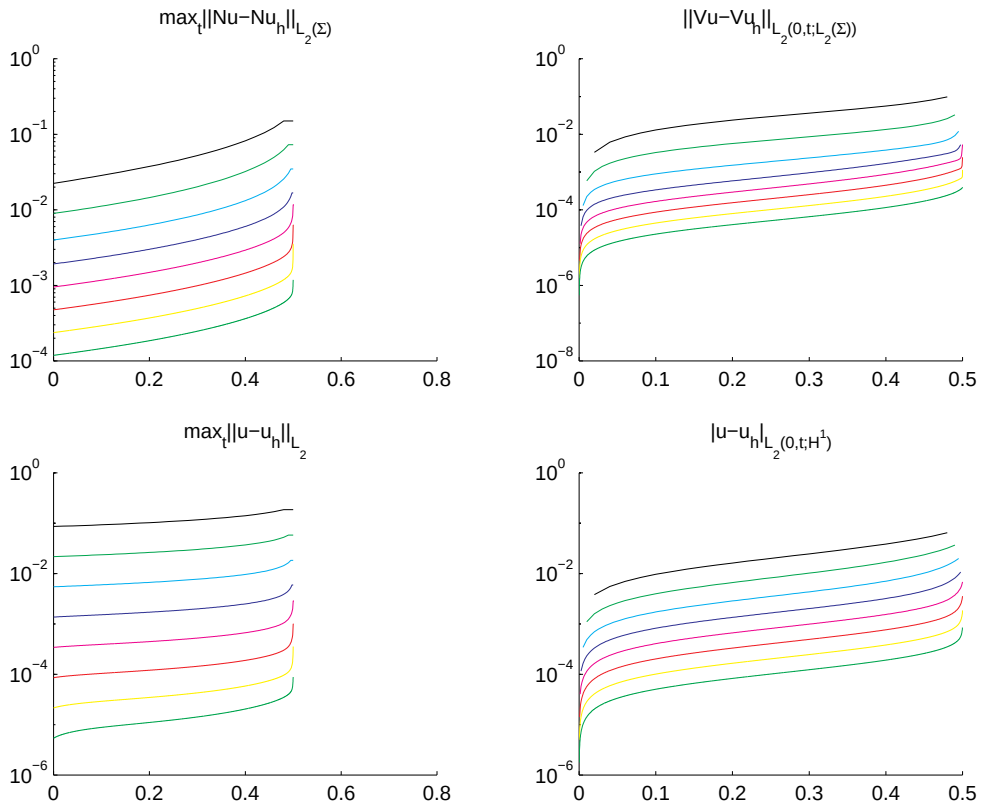

Figure 4.9: We report the error measured with the geometric quantities and the Sobolev norms for the shrinking sphere example. Different colors stand for different meshsizes $h \in \{1.0000, 0.5000, 0.2500, 0.1250, 0.0625, 0.0312, 0.0156, 0.0078\}$ and the abscissa is the time variable. Again the use of geometric quantities does not compromise our results as they behave very similarly to norms as far as convergence is concerned.

In this example the error increases as t reaches 0.5, the boundary blow-up point.

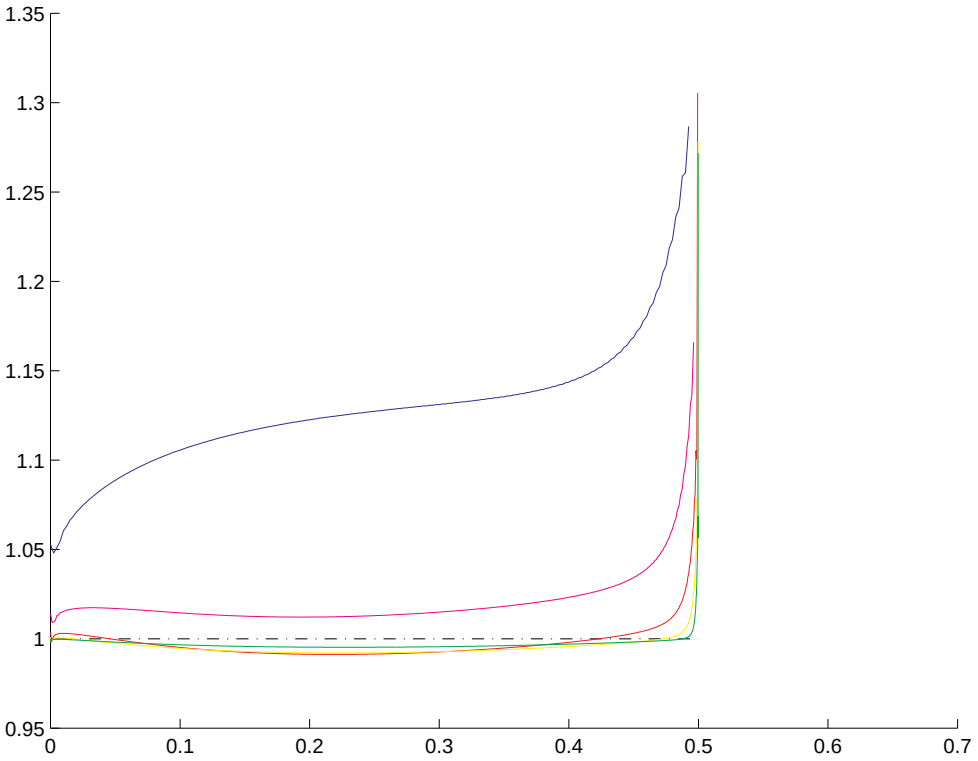

Figure 4.10: The EOC of the geometric error E gets close to 1 . This is the rate that is expected in theory. In these plots the rate seems to be slightly better than 1 in a first stage. Different colors stand for different meshsizes $h \in \{1.0000, 0.5000, 0.2500, 0.1250, 0.0625, 0.0312, 0.0156, 0.0078\}$ and the abscissa is the time variable. Notice the dramatic change of behavior near the blow-up time $t = 0.5$.

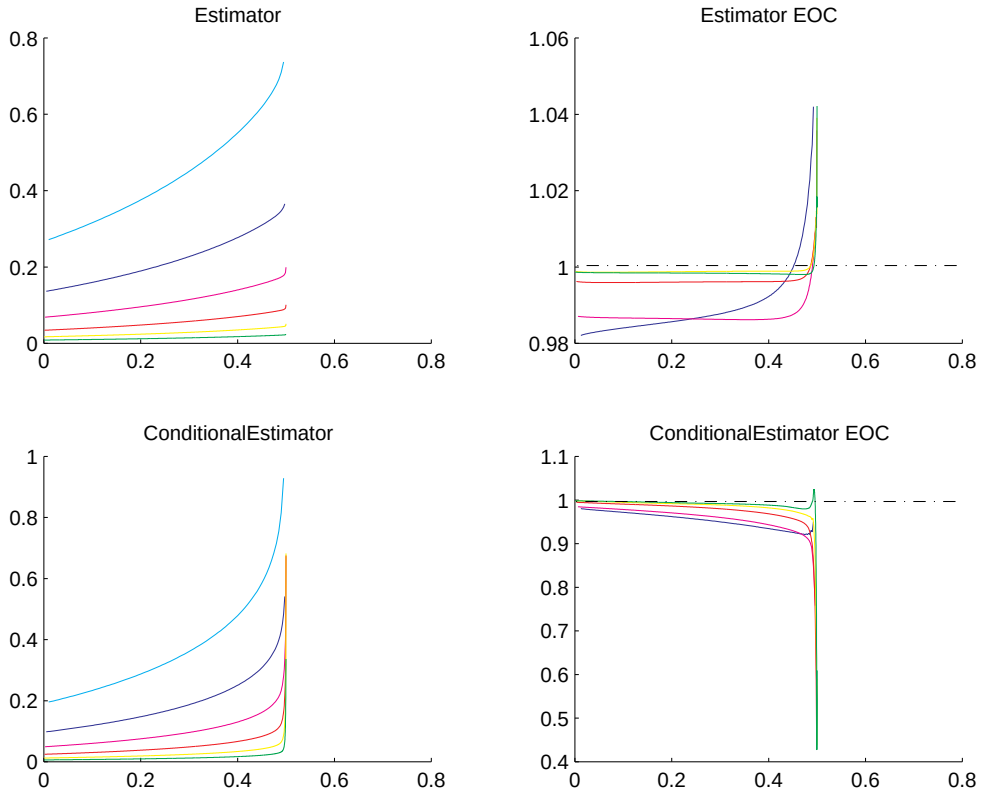

Figure 4.11: In these plots we exhibit on the left-hand side both the proper estimator $\widehat{\mathscr{E}}$ and the conditional estimator $\mathscr{E}_\infty$. Their EOC is computed and plotted on the right hand side. Different colors stand for different meshsizes $h \in \{1.0000, 0.5000, 0.2500, 0.1250, 0.0625, 0.0312, 0.0156, 0.0078\}$ and the abscissa is the time variable. As before we see that $\widehat{\mathscr{E}}$ converges with an asymptotic rate of 1. Again the discrepancy between the EOC for the proper and conditional estimators is striking. There is a striking difference between $\widehat{\mathscr{E}}$ and $\mathscr{E}_\infty$ near the blow-up time $t = 0.5$. The proper estimator $\widehat{\mathscr{E}}$ follows the behavior of the error E itself, while the conditional estimator $\mathscr{E}_\infty$ performs worse and worse as we inch toward the blow-up.

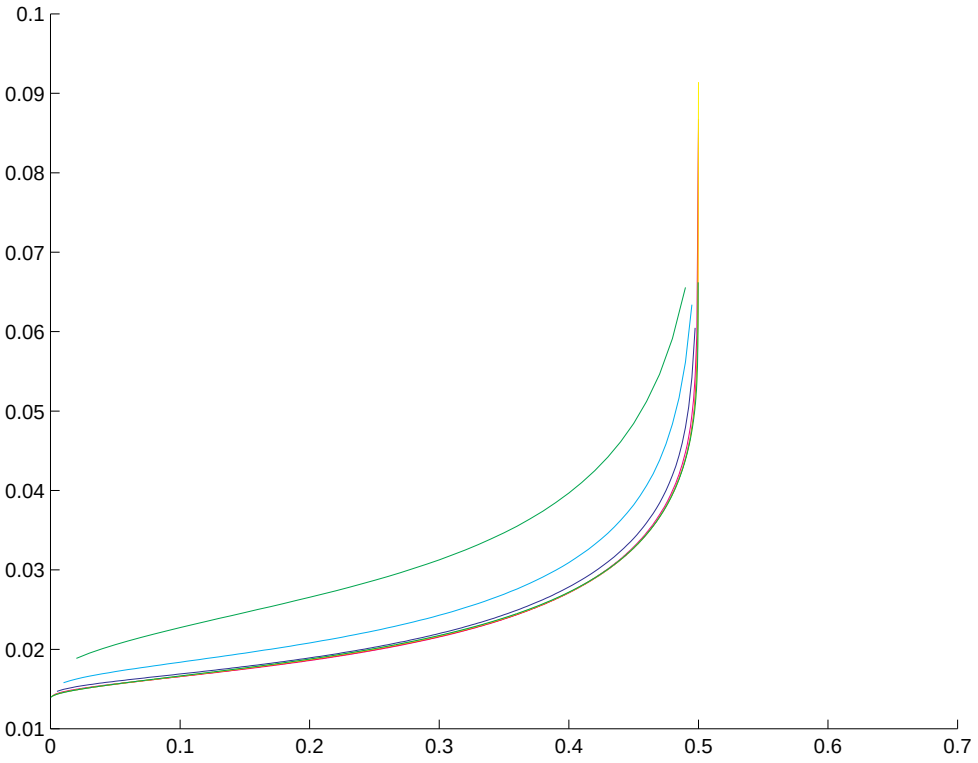

Figure 4.12: This plot represents the ratio between the exact error E and the estimator $\widehat{\mathscr{E}}$. Different colors stand for different meshsizes $h \in \{1.0000, 0.5000, 0.2500, 0.1250, 0.0625, 0.0312, 0.0156, 0.0078\}$ and the abscissa is the time variable. This is a crucial test for the estimators, the fact that the ratio converges as $h \to 0$ to a function of time means that the asymptotic behavior of the error and the estimator are the same. The theory derived in Chapter 3 gives a worst case scenario prediction of a ratio that is an increasing exponential. In this case we see that the ratio increases dramatically as t reaches 0.5, the blow-up point. (The last numerical solution $u_{0.0078}$ doesn't have it's ratio plotted for the last point, as it is a very big number.)

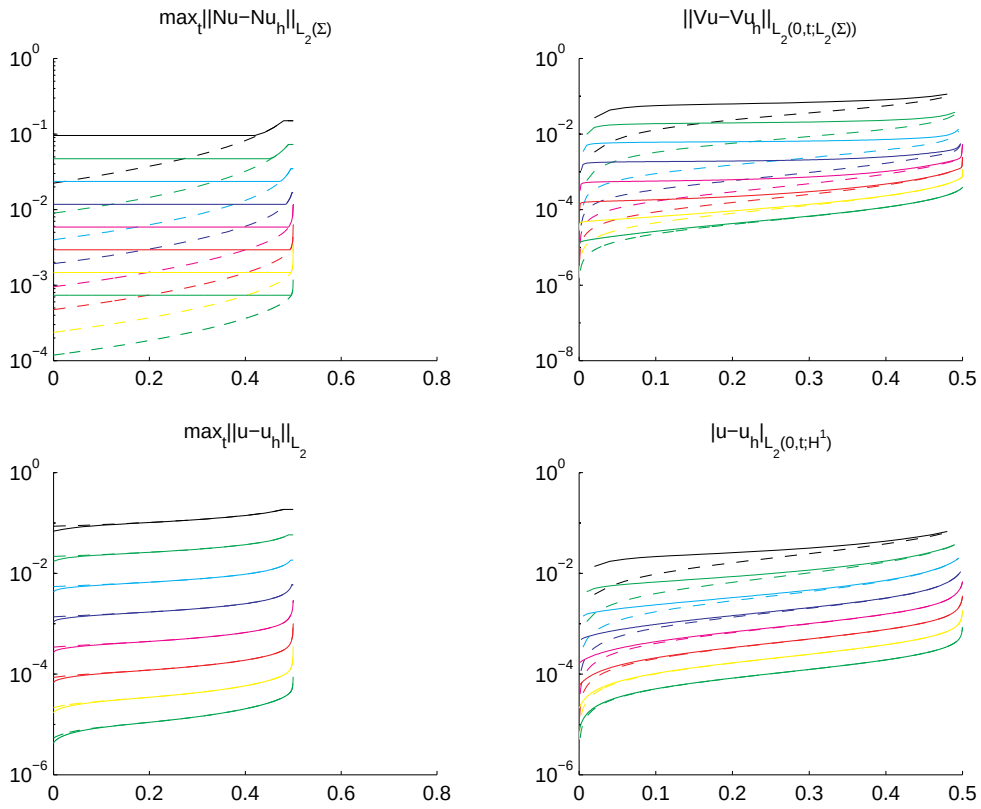

Figure 4.13: In this picture we have plotted simultaneously the errors in various norms for the shrinking sphere simulations in two different cases. The dashed lines correspond to the situation we presented above, where the initial condition is approximated through a minimal surface projection (4.15), while the solid lines correspond to the solution with a simple nodal Lagrange interpolant. The initial part of the interval shows how bad can be the second choice with respect to the first one. Recall that in the shrinking sphere there is nothing special about starting at time 0.0, the solution is somewhat self similar and the error is bound to get worse as time goes on, assuming that the initial condition is well resolved.

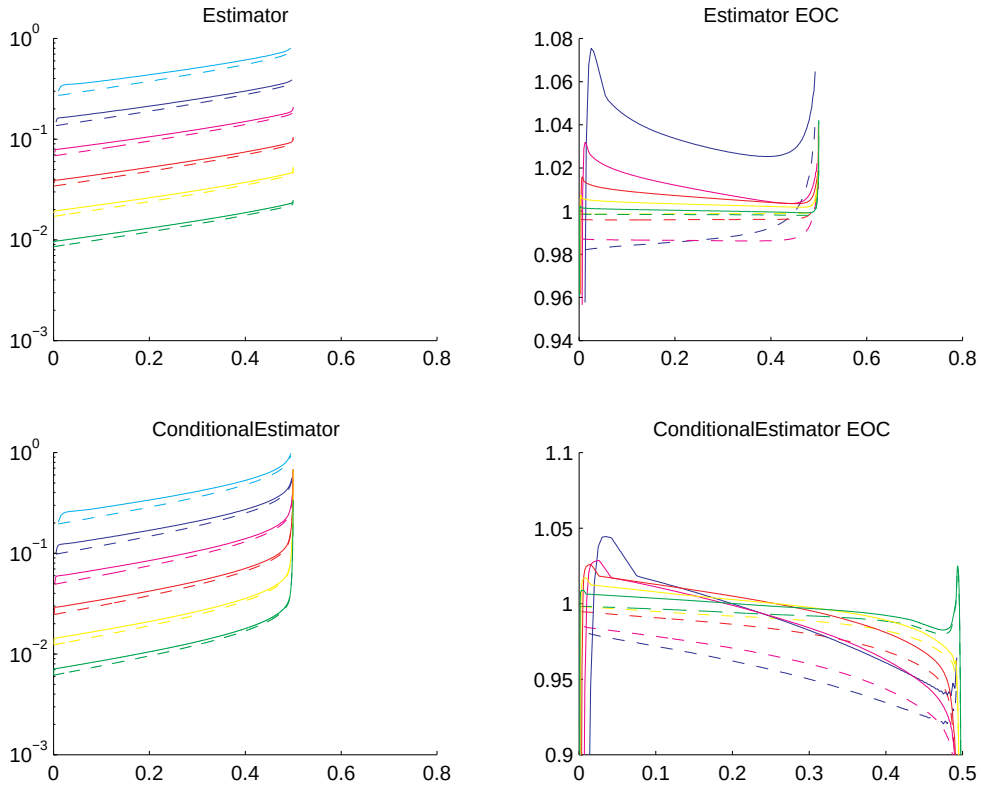

Figure 4.14: In this picture we have plotted simultaneously the estimators and their EOC, in various norms for the shrinking sphere simulations in two different cases. The dashed lines correspond to the situation we presented above, where the initial condition is approximated through a minimal surface projection (4.15), while the solid lines correspond to the solution with a simple nodal Lagrange interpolant. Notice however the EOC when we use the Lagrange interpolant. It is better than the one for the minimal surface. This is probably due to the fact that the effect of choosing the former is reduced as the meshsize goes to zero.

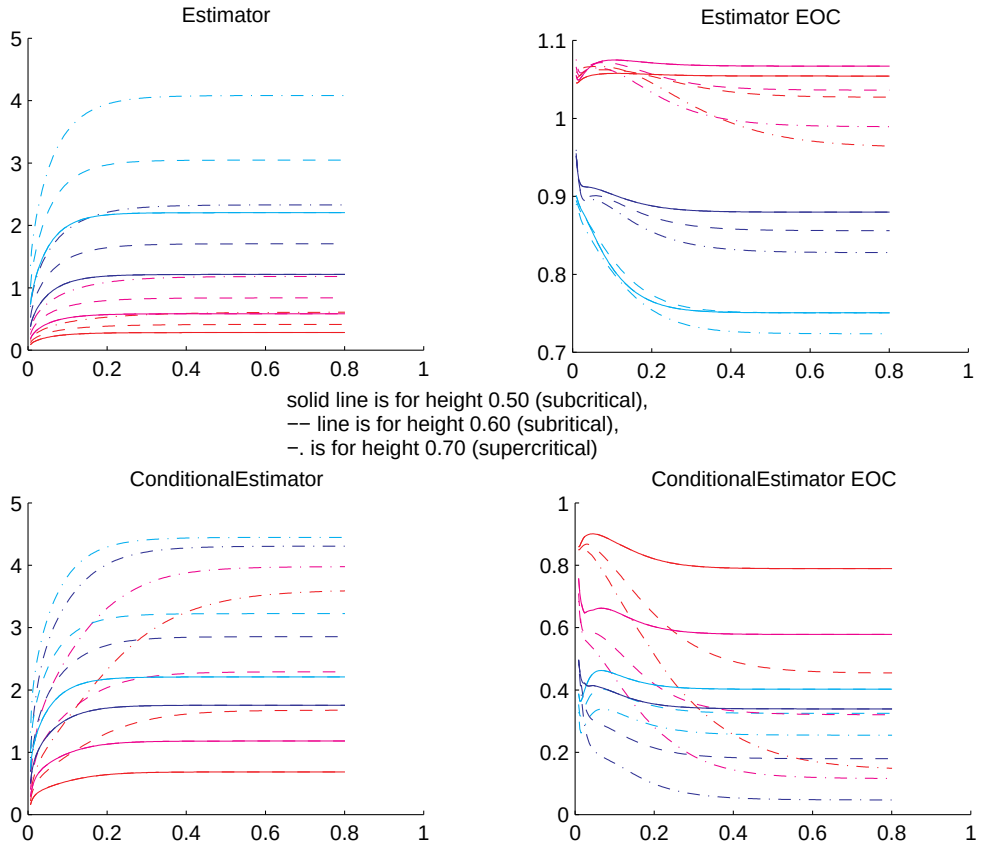

Figure 4.15: These are the estimators for the catenoid problem for different heights $H = 0.50, 0.60, 0.70$ (line style) and different meshsizes $h \in \{0.1571, 0.0798, 0.0402, 0.0202\}$ (color). A noteworthy feature of these computations is the behavior of the EOC, especially for the conditional estimator. As H increases this estimator which is well behaved at initial times, gets into a poor convergence regime. This means that the conditional estimators might not be applicable for the cases where H is supercritical. In this case a blow up occurs in finite time [Ura94]. The poor behavior of the conditional estimator can be interpreted as an indication of this phenomenon.

Appendix A

A.1 Notation and conventions

Sets and functions

The sets $\mathbb{Z}$, $\mathbb{R}$ and $\mathbb{C}$ are the customary sets of integer, real and complex numbers respectively. The set of natural numbers (the strictly positive integers) is denoted by $\mathbb{Z}^+$. We also use the set of natural numbers and zero $\mathbb{N}_0 := \mathbb{Z}^+ \cup \{0\}$. The same convention is applied to the real numbers, so $\mathbb{R}^+$ and $\mathbb{R}_0^+$ indicate the open and the closed positive real axes, respectively.

To indicate segments of integers we borrow the notation partially from Matlab®; that is, given two integers $i, j \in \mathbb{Z}$, we define

$$[i : j] := \{k \in \mathbb{Z} : i \leq k \leq j\},$$

$$[i :] := \{k \in \mathbb{Z} : i \leq k\},$$

$$[: i] := \{k \in \mathbb{Z} : k \leq i\}.$$

For $a, b \in \mathbb{R}$ the closed interval is denoted by $[a, b]$ and the open interval by (a, b). Parentheses and square brackets are combined also to define semi-open intervals like $[0, T)$.

If $d \in \mathbb{Z}^+$, $\mathbb{R}^d$ denotes the d-dimensional real vector space. Unless otherwise stated it is assumed that $\mathbb{R}^d$ is equipped with the euclidean structure. We use the notation $x \cdot y$ for the inner product in $\mathbb{R}^d$ and the euclidean norm is denoted by $|x|$.

The open ball centered at $x \in \mathbb{R}^d$ with radius $r \in \mathbb{R}^+$ is denoted by $\mathrm{B}_r(x)$. If the dimension needs to be specified then the ball is denoted by $\mathrm{B}_r^d(x)$.

A.1.1 Definition (Space-time)**.** Given a spatial domain $\Omega \in \mathbb{R}^d$ and a time interval (T_0, T), the corresponding *time-space cylinder* is the cartesian product $\Omega \times (T_0, T)$. The *parabolic boundary* of the time-space cylinder $\Omega \times (T_0, T)$ is defined as follows

$$\partial_{\mathrm{p}}(\Omega \times (T_0, T)) := (\Omega \times T_0) \cup (\partial\Omega \times (T_0, T)).$$

For functions defined on a space-time domain, dependence on the spatial variable is often omitted. For instance, in many cases $f(t)$ stands for the function $\Omega \ni x \mapsto f(x,t)$. We adopt this notation because it should not be a source of major problems, while it improves readability and saves some space in long formulas.

A.1.2 Definition (Differential symbology)**.** Let $D \in \mathbb{R}^N$ be an open set and $y \in D$. Given a function $f : D \to \mathbb{R}$ and a field $\boldsymbol{w} : D \to \mathbb{R}^N$ we use the following notation:

- The *first derivative* of f at a point $y \in D$ (a linear form on $\mathbb{R}^n$ at each point of D) is denoted by $\partial f(y)$.
- The *first derivative* of $\boldsymbol{w}$ at a point $y \in D$ (a linear operator from $\mathbb{R}^n$ into $\mathbb{R}^n$) is denoted by $\partial \boldsymbol{w}(y)$.

- The *gradient* of f at y (defined as the Riesz representative of $\partial f(y)$ with respect to the usual euclidean structure) is denoted by $\nabla f(y)$.
- Similarly, the *Jacobian* of $\boldsymbol{w}$ at y is denoted by $\nabla \boldsymbol{w}(y)$.
- The *first partial derivative in the n-th direction* is denoted by $\partial_n f$;
- The *second order derivative* is indicated by $\partial^2 f$ and the *second order partial derivative in the n-th and m-th directions* by $\partial_{n,m} f$ (or $\partial_n^2 f$, when $n = m$.)
- According to this notation the *Hessian* of f should be written as $\nabla^2 f$, but we often denote it with $\partial^2 f$ in order not to confuse it with the *Laplacian* which is denoted with Δf.
- Given a multi-index $\alpha = (\alpha_1, \ldots, \alpha_N) \in \mathbb{N}_0^N$, then $\partial^\alpha f = \partial^{\alpha_1} \cdots \partial^{\alpha_N} f$.

A.1.3 Definition (Space-time differential symbology)**.** When dealing with space time functions, that is, in the particular case where $D = \Omega \times (0, T) \in \mathbb{R}^{d+1}$ is a space-time cylinder and f a function that might depend on space and time we will use a somewhat abusive[1]) variation of the definitions in A.1.2:

- No subscript in front of the differential operators mean derivatives with respect to the space variable. For example, the *space derivative* is indicated with ∂f, the *space gradient* corresponding to ∂f is denoted by ∇f and so forth respecting the convention in.
- the *partial space derivative in i-th (spatial) direction* is denoted by $\partial_i u$.
- the *time derivative* is denoted by $\partial_t u$ (even when time variable is indicated by some other symbol!);

[1]Examples of this abuse are $\int_0^t \partial_t f(x, s)\, \mathrm{d}s$ or $\partial^2 f(t)$.

- iterated derivatives in space (or time) are denoted by "powers" like $\partial^2 u$ or $\partial_t^2 u$
- mixed space-time derivatives use two different symbols like $\partial_t \partial_i u$ or $\partial_t \nabla u$.

These definitions can be extended to subsets of the closure of open sets by continuity. We will use such extension and will not need further generalization.

Function spaces

We use function spaces only on bounded (space, time, and space-time) Lipschitz domains [EG92]. Space and time variables have sometimes different indices.

A.1.4 Definition (Lipschitz and C^k domain)**.** An open set $D \subset \mathbb{R}^N$ is said to be a *Lipschitz domain* if it satisfies the definition in Evans & Gariepy book [EG92, Section 4.2, p. 127]. For $k \in \mathbb{Z}^+$, a Lipschitz domain D is said to be a C^k *domain* if and only if its boundary ∂D is a finite union of C^k manifolds.

A.1.5 Definition (Spaces of (Hölder) continuous functions)**.** Let D be a bounded domain in $\mathbb{R}^N$, $k \in \mathbb{Z}^+$, $s \in \mathbb{R}^+ \setminus \mathbb{Z}^+$, we adopt the following notation

$$\mathrm{C}(D) = \mathrm{C}^0(D) := \{f : D \to \mathbb{R} : \ f \text{ is continuous on } D\}$$

$$\mathrm{C}^k(D) := \left\{f : D \to \mathbb{R} : \ \partial^\alpha f \in \mathrm{C}(D),\ \forall \alpha \in \mathbb{N}_0^N,\ |\alpha| \le k\right\}$$

$$\mathrm{C}^s(D) := \left\{ f \in \mathrm{C}^{[s]} : \ \sup_{x,y \in D} \frac{|\partial^\alpha f(x) - \partial^\alpha f(y)|}{|x-y|^{\{s\}}} < \infty,\ \forall \alpha \in \mathbb{N}_0^N, |\alpha| = [s] \right\}.$$

Here $[s]$ is the *integer part* of s, i.e., the largest integer that is smaller than s, and $\{s\} = s - [s]$ is the *fractional part*.

The space of smooth functions is given by $\mathrm{C}^\infty(\Omega) = \bigcap_{k=1}^\infty \mathrm{C}^k(\Omega)$, and the space of compactly supported smooth functions is denoted by $\mathrm{C}_\mathrm{c}^\infty(\Omega)$.

Similarly we have

$$\text{(A.1)} \qquad \mathrm{C}(\overline{D}) = \mathrm{C}^0(\overline{D}) := \{f : D \to \mathbb{R} : \ f \text{ is uniformly continuous on } D\}$$

and so forth.

A.1.6 Definition (Sobolev spaces)**.** Let $D \in \mathbb{R}^N$, and $k \in \mathbb{Z}^+$. The usual spaces of Lebesgue integrable functions are denoted by $\mathrm{L}_p(D)$, for $p \in [1, \infty]$. We take the space of *k-times weakly differentiable functions* W^k as defined in [GT83, sec. 7.3, p. 149]. Finally the *Sobolev spaces* are defined as usual

$$\mathrm{W}^k_p(D) = \left\{ f \in \mathrm{W}^k(D) : \ \partial^\alpha f \in \mathrm{L}_p(D), \ \forall \alpha \in \mathbb{N}_0^N, |\alpha| \le k \right\},$$

$$\mathring{\mathrm{W}}^k_p(D) = \mathrm{closure}_{\mathrm{W}^k_p(D)} \, \mathrm{C}^\infty_{\mathrm{c}}(D).$$

A.1.7 Definition (Space-time function spaces)**.** If $D = \Omega \times (0, T) \subset \mathbb{R}^{d+1}$, sometimes we need to consider spaces where the smoothness order in the spatial derivative differs from the one in the time derivative. Namely

$$\begin{aligned} \mathrm{C}^{k,l}(\Omega \times (0,T)) = \Big\{ & f : \Omega \times (0,T) \to \mathbb{R} : \\ & \partial^\alpha f \in \mathrm{C}(\Omega \times (0,T)), \ \forall \alpha \in \mathbb{N}_0^d, |\alpha| \le k \\ & \text{and } \partial_t^j f \in \mathrm{C}(\Omega \times (0,T)), \ \forall j \in [0 : \ell] \Big\} \end{aligned}$$

All the definitions above apply (with the appropriate modifications) to spaces of functions which take values in a Banach space, instead of $\mathbb{R}$.

A.2 Simple technical tools

The following is the version of Gronwall inequality that we shall use. Although it can be found in many textbooks we include the proof.

A.2.1 Lemma (Gronwall inequality). *Let $T \in \mathbb{R}^+$ and f, g, k, l be real-valued measurable functions defined on $[0,T]$, such that:*

(a) k and l are non-negative;

and

(b) $$l(t) + f(t) \leq g(t) + \int_0^t k(s) f(s)\,\mathrm{d}s < \infty, \quad \forall t \in [0,T].$$

Then

$$l(t) + f(t) \leq \sup_{s\in[0,t]} |g(s)| \exp \int_0^t k(s)\,\mathrm{d}s, \quad \forall t \in [0,T]. \tag{A.2}$$

Proof Introduce $F(t) = \int_0^t k(s) f(s)\,\mathrm{d}s$ and $K(t) = \int_0^t k(s)\,\mathrm{d}s$. Then from (b) and the non-negativity of k and l we infer

$$\begin{aligned}\frac{\mathrm{d}}{\mathrm{d}t}\left(\mathrm{e}^{-K(t)}\, F(t)\right) &= \mathrm{e}^{-K(t)}\, k(t) f(t) - \mathrm{e}^{-K(t)}\, k(t) \int_0^t k(s) f(s)\,\mathrm{d}s \\ &\leq \mathrm{e}^{-K(t)}\, k(t) g(t).\end{aligned}$$

An integration on $[0,t]$ and the use of assumption (a), yields

$$\begin{aligned}\mathrm{e}^{-K(t)}\, F(t) &\leq \int_0^t \mathrm{e}^{-K(s)}\, k(s) g(s)\,\mathrm{d}s \\ &\leq \sup_{s\in[0,t]} |g(s)| \int_0^t \mathrm{e}^{-K(s)}\, k(s)\,\mathrm{d}s \\ &= -\sup_{s\in[0,t]} |g(s)| \int_0^t \frac{\mathrm{d}}{\mathrm{d}s}\, \mathrm{e}^{-K(s)}\,\mathrm{d}s \\ &= \sup_{s\in[0,t]} |g(s)| \left(1 - \mathrm{e}^{-K(t)}\right).\end{aligned}$$

Thus $F(t) \leq \sup_{[0,t]} |g| \left(\mathrm{e}^{K(t)} - 1\right)$. Combining this with assumption (b) we obtain the bound for $l(t) + f(t)$. □

A.2.2 Theorem (Gauss-Green formula). *Let Ω be a Lipschitz domain. Sup-*

pose $\boldsymbol{w} \in \mathrm{W}^1_p(\Omega)^d$ *and* $z \in \mathrm{W}^1_{p'}(\Omega)$ *where* p' *is the conjugate exponent*[2]*, for some* $p \in [1, \infty]$*, then we have*

$$\int_\Omega \nabla z(x) \cdot \boldsymbol{w}(x) + \int_\Omega z(x) \operatorname{div} \boldsymbol{w}(x) \,\mathrm{d}x = \int_{\partial\Omega} z(x) \boldsymbol{w}(x) \cdot \boldsymbol{\nu}(x) \,\mathrm{s}(\mathrm{d}x) \tag{A.3}$$

Proof For each $i \in [1 : d]$ we apply the product rule for conjugate Sobolev spaces and the integration by parts rule [EG92, 4.3, The. 1(ii)] with $zw_i \in \mathrm{W}^1_1(\Omega)$ as the Sobolev function and $(\delta^i_j)_j$ as the test vector field. This yields

$$\begin{aligned}\int_\Omega z(x)\partial_i w_i(x) + \partial_i z(x) w_i(x) \,\mathrm{d}x &= \int_\Omega \partial_i (z(x) w_i(x)) \,\mathrm{d}x \\ &= \int_{\partial\Omega} z(x) w_i(x) \nu_i(x) \,\mathrm{s}(\mathrm{d}x).\end{aligned}$$

Summing over $i \in [1 : d]$ we obtain the result. □

Clément-Scott-Zhang interpolation

We will be often using interpolation of weakly differentiable functions (like W^1_2) into finite element spaces, so Lagrange interpolation is not powerful enough and we need to use regularized interpolation like the one discussed by Clément in his PhD dissertation [Clé75]. Since we also require some care with the boundary values, like preserving homogeneity, we will be dealing with a refinement of Clément interpolation, namely the boundary value preserving and projection interpolation introduced by Scott & Shangyou Zhang [SZ90]. The needed results can be summarized in the following[3]

---

[2]By *conjugate exponent* we mean the usual $p' = p/(p-1)$, if $p \in (1, \infty)$, and $p' = \infty$ (resp. 1), if $p = 1$ (resp. ∞).

[3]We use the notation introduced in section 2.5.

A.2.3 Theorem ([SZ90, Theorem 2.1 and eqn. (4.3)])**.** *There exists a linear operator*

$$I_h : \mathrm{W}_1^1(\Omega) \to \mathbb{V}_h^\ell \tag{A.4}$$

that satisfies the following properties

$$I_h|_{\mathbb{V}_h^\ell} = \mathrm{id}_{\mathbb{V}_h^\ell} \text{ (projection property);} \tag{A.5}$$

$$I_h(\mathring{\mathrm{W}}_1^1(\Omega)) = \mathring{\mathbb{V}}_h^\ell \text{ (boundary value preservation);} \tag{A.6}$$

$$\|v - I_h v\|_{\mathrm{W}_p^m(K)} \le C(d,\ell,\sigma_0) h_K^{1-m} \, |v|_{\mathrm{W}_p^1(\mathscr{U}_K^h)}, \ \forall v \in \mathrm{W}_p^1(\mathscr{U}_K^h), K \in \mathscr{T}_h; \tag{A.7}$$

$$\|v - I_h v\|_{\mathrm{L}_p(\partial K)} \le C'(d,\ell,\sigma_0) h_K^{1-1/p} \, |v|_{\mathrm{W}_p^1(\mathscr{U}_K^h)}, \ \forall v \in \mathrm{W}_p^1(\mathscr{U}_K^h), K \in \mathscr{T}_h. \tag{A.8}$$

Here $m \in \{0,1\}$, $p \in [1,\infty)$ and $\mathscr{U}_K^h$ denotes the union of all simplexes that are neighbors of K in the triangulation $\mathscr{T}_h$.

Proof The first three properties are just copied from equations [SZ90, (2.17), (2.18) and (4.3)]. To prove (A.8), we use the trace inequality [EG92, sec. 4.3] on the reference simplex $\hat{K}$ and a standard scaling argument by taking $\hat{K}$ into K by using a Lipschitz piecewise linear transformation $X_h : \mathscr{U}_{\hat{K}} \to \mathscr{U}_K^h = X(\hat{K})$. We obtain

$$\begin{aligned}
\|v - I_h v\|_{\mathrm{L}_p(\partial K)} &= \left(\int_{\partial K} |v(x) - I_h v(x)|^p \, \mathrm{d}x \right)^{1/p} \\
&= \left(\int_{\partial K} \left| \hat{v}(X_h^{-1}(x)) - \hat{I}\hat{v}(X_h^{-1}(x)) \right|^p \mathrm{d}x \right)^{1/p} \\
&= \left(\int_{\partial \hat{K}} \left| \hat{v}(x) - \hat{I}\hat{v}(x) \right|^p |\det \nabla X_h(x)| \, \mathrm{d}x \right)^{1/p} \\
&\le C(\sigma_0) h^{(d-1)/p} \left\| \hat{v} - \hat{I}\hat{v} \right\|_{\mathrm{L}_p(\partial \hat{K})} \\
&\le C'(\sigma_0) h^{(d-1)/p} \left\| \hat{v} - \hat{I}\hat{v} \right\|_{\mathrm{W}_p^1(\hat{K})}
\end{aligned}$$

$$\leq C(p,\ell,\sigma_0)C'(\sigma_0)h^{(d-1)/p}\,|\hat{v}|_{\mathrm{W}^1_p(\mathscr{U}_{\hat{K}})}\,.$$

The last step owes to (A.7). We conclude by rescaling back

$$|\hat{v}|_{\mathrm{W}^1_p(\mathscr{U}_{\hat{K}})} \leq C(\sigma_0)h^{(p-d)/p}\,|v|_{\mathrm{W}^1_p(\mathscr{U}^h_K)} \tag{A.9}$$

and piecing together the last two inequalities. □

We need also a version of (A.7) where the integrability indices are different. This version uses the Sobolev imbedding theorem

A.2.4 Corollary. *Given the Scott-Zhang interpolation operator I_h, $p,q \in [1,\infty)$ such that*

$$q \leq \frac{dp}{d-p};$$

then the following inequality holds

$$\|v - I_h v\|_{\mathrm{L}_q(K)} \leq C(d,p,\ell,\sigma_0)h^{1-d/p+d/q)}\,|v|_{\mathrm{W}^1_p(\mathscr{U}^h_K)}\,. \tag{A.10}$$

Proof In view of the Sobolev inequality [GT83] we have

$$\left\|\hat{v} - \hat{I}\hat{v}\right\|_{\mathrm{L}_q(\hat{K})} \leq C(p,d)\left\|\hat{v} - \hat{I}\hat{v}\right\|_{\mathrm{L}_p(\hat{K})}, \tag{A.11}$$

where $\hat{K}$ is the reference simplex as in the proof of Theorem A.2.3. Complete this inequality by using (A.7) and obtain

$$\left\|\hat{v} - \hat{I}\hat{v}\right\|_{\mathrm{L}_q(\hat{K})} \leq C(d,p,\ell,\sigma_0)\,|\hat{v}|_{\mathrm{W}^1_p(\mathscr{U}_{\hat{K}})}\,. \tag{A.12}$$

A scaling argument as in proof of A.2.3 gives

$$\|v - I_h v\|_{\mathrm{L}_q(K)} \leq C'(\sigma_0)h^{d/q}\left\|\hat{v} - \hat{I}\hat{v}\right\|_{\mathrm{L}_q(\hat{K})},$$

and

$$|\hat{v}|_{\mathrm{W}^1_p(\mathscr{U}_{\hat{K}})} \leq C'(\sigma_0)h^{(p-d)/p}\,|v|_{\mathrm{W}^1_p(\mathscr{U}^h_K)}\,.$$

The proof is concluded by assembling together the last three inequalities. □

A.3 An aposteriori error bound for the heat equation in higher Sobolev norms

In this section we derive an aposteriori error bound for the Cauchy-Dirichlet problem associated to the heat equation

$$\partial_t u - \Delta u = 0, \text{ in } \Omega \times (0,T], \tag{A.13}$$

$$u = g, \text{ on } \partial_{\mathrm{p}}\left(\Omega \times (0,T)\right). \tag{A.14}$$

Although the purpose of this exercise is to outline part of the proof in chapter 3, it should be mentioned that this simple result is inedited to the best of our knowledge.

We combine an energy and residual technique to derive our bound. The basic energy estimate, however, is not for the customary norms

$$\sup_{[0,T]} \|u\|^2_{\mathrm{L}_2(\Omega)} + \int_0^t \|\nabla u\|^2_{\mathrm{L}_2(\Omega)}, \tag{A.15}$$

but rather for the stronger *higher order norms*

$$\int_0^T \|\partial_t u\|^2_{\mathrm{L}_2(\Omega)} + \sup_{[0,T]} \|\nabla u\|^2_{\mathrm{L}_2(\Omega)}. \tag{A.16}$$

The reason for this is that, rather than testing equation (A.13) with u, we test it with $\partial_t u$.

Rewrite the problem into the weak form

$$\langle \partial_t u, \phi\rangle + \langle \nabla u, \nabla \phi\rangle = 0, \ \forall \phi \in \overset{\circ}{\mathrm{W}}{}^1_2, \tag{A.17}$$

with $u - g \in \overset{\circ}{\mathrm{W}}{}^1_2$ and $u(0) = g(0)$. Then borrowing the finite element notation from section 2.5, introduce the spatial finite element discretization

$$\langle \partial_t u_h, \phi_h\rangle + \langle \nabla u_h, \nabla \phi_h\rangle = 0, \ \forall \phi_h \in \overset{\circ}{\mathbb{V}}{}^\ell_h \tag{A.18}$$

with $u_h - g \in \mathring{\mathbb{V}}_h^\ell$. (For simplicity we assume that the boundary data is time independent.)

Galerkin orthogonality implies the error equation

$$\langle \partial_t u_h - \partial u, \phi \rangle + \langle \nabla u_h - \nabla u, \nabla \phi \rangle = \langle \partial_t u_h, \phi - \phi_h \rangle + \langle \nabla u_h, \nabla \phi - \nabla \phi_h \rangle \,, \tag{A.19}$$

for all $\phi \in \mathring{\mathrm{W}}_2^1$ and $\phi_h \in \mathring{\mathbb{V}}_h^\ell$.

Let $e = u_h - u$ be the error and take $\phi = \partial_t e$. Since the boundary data is time independent, ϕ is in $\mathring{\mathrm{W}}_2^1$ and is thus admissible. On the other hand, we let $\phi_h = I_h \phi$ where I_h is the Scott-Zhang interpolator defined in Theorem A.2.3. Then (A.19) and an integration in time yield

$$\begin{aligned} &\int_0^t \|\partial_t e\|_{\mathrm{L}^2}^2 + \frac{1}{2} \|\nabla e(t)\|_{\mathrm{L}^2}^2 - \frac{1}{2} \|\nabla e(0)\|_{\mathrm{L}^2}^2 \\ &\qquad = \int_0^t \|\partial_t e(s)\|_{\mathrm{L}^2}^2 + \frac{1}{2} \,\mathrm{d}_t \|\nabla e(s)\|_{\mathrm{L}^2}^2 \,\mathrm{d}s \\ &\qquad = \int_0^t \langle \mathscr{R}(s) \,|\, \partial_t (e(s) - I_h e(s)) \rangle \,\mathrm{d}s \end{aligned} \tag{A.20}$$

where the residual functional $\mathscr{R} \in \mathrm{W}_2^{-1}(\Omega)$ can be represented as

$$\begin{aligned} \langle \mathscr{R} \,|\, \psi \rangle &= \langle \partial_t u_h, \psi \rangle + \langle \nabla u_h, \psi \rangle \\ &= \sum_{K \in \mathscr{T}_h} \langle \partial_t u_h - \Delta u_h, \psi \rangle_K + \frac{1}{2} \langle [\![\nabla u_h]\!] \,, \psi \rangle_{\partial K \cap \Omega} \quad =: \langle r, \psi \rangle + \langle j, \psi \rangle_{\Sigma_h} \,. \end{aligned}$$

for all $\psi \in \mathring{\mathrm{W}}_2^1(\Omega)$.

To estimate the residual we use Fubini theorem to interchange the space and time integrals and integrate by parts in time. We abbreviate the writing by doing

this rather formally

$$\begin{aligned}
&\int_0^t \langle \mathscr{R}(s) \,|\, \partial_t(e(s) - I_h e(s)) \rangle \, \mathrm{d}s \\
&= \langle \mathscr{R}(t) \,|\, e(t) - I_h e(t) \rangle - \langle \mathscr{R}(0) \,|\, e(0) - I_h e(0) \rangle \\
&\quad - \int_0^t \langle \partial_t \mathscr{R}(s) \,|\, e(s) - I_h e(s) \rangle
\end{aligned} \tag{A.21}$$

Now we need to estimate all these terms to factor out $|e|_{\mathrm{W}_2^1}$. This is easily achieved by using the properties of operator I_h given in Theorem A.2.3. For instance, we have

$$\begin{aligned}
\langle \partial_t \mathscr{R} \,|\, e - I_h e \rangle &= \langle \partial_t r, e - I_h e \rangle + \langle \partial_t j, e - I_h e \rangle_{\Sigma_h} \\
&= \left\langle h \partial_t r, h^{-1}(e - I_h e) \right\rangle + \left\langle h^{1/2} \partial_t j, h^{-1/2}(e - I_h e) \right\rangle_{\Sigma_h} \\
&\leq \|h \partial_t r\|_{\mathrm{L}_2(\Omega)} \left\| h^{-1}(e - I_h e) \right\|_{\mathrm{L}_2(\Omega)} \\
&\quad + \left\| h^{1/2} \partial_t j \right\|_{\mathrm{L}_2(\Sigma_h)} \left\| h^{-1/2}(e - I_h e) \right\|_{\mathrm{L}_2(\Sigma_h)} \\
&\leq \left(C \|h \partial_t r\|^2_{\mathrm{L}_2(\Omega)} + C' \left\| h^{1/2} \partial_t j \right\|^2_{\mathrm{L}_2(\Sigma_h)} \right)^{1/2} \|\nabla e\|_{\mathrm{L}_2(\Omega)} .
\end{aligned}$$

Here $C = C(d, l, \sigma_0)$, $C' = C'(d, l, \sigma_0)$ are the constants appearing in Theorem A.2.3.

Combining estimations of this type with (A.21) and (A.20) we obtain

$$\begin{aligned}
\int_0^t \|\partial_t e\|^2_{\mathrm{L}_2(\Omega)} + \frac{1}{2} \|\nabla e(t)\|^2 &\leq \|\nabla e(0)\|^2 + \frac{1}{2} \left(C \|h r(0)\|^2_{\mathrm{L}_2(\Omega)} + C' \left\| h^{1/2} j(0) \right\|^2_{\mathrm{L}_2(\Sigma_h)} \right) \\
&\quad + \mu \|\nabla e(t)\|^2_{\mathrm{L}_2(\Omega)} + \frac{1}{4\mu} \left(C \|h r(t)\|^2_{\mathrm{L}_2(\Omega)} + C' \left\| h^{1/2} j(t) \right\|^2_{\mathrm{L}_2(\Sigma_h)} \right) \\
&\quad + \mu \sup_{[0,t]} \|\nabla e(t)\|^2_{\mathrm{L}_2(\Omega)} + \frac{1}{4\mu} \left(\int_0^t \left(C \|h \partial_t r\|^2_{\mathrm{L}_2(\Omega)} + C' \left\| h^{1/2} \partial_t j \right\|^2_{\mathrm{L}_2(\Omega)} \right)^{1/2} \right)^2 ,
\end{aligned}$$

where the arbitrary parameter $\mu > 0$ is to be fixed.

If we fix now a time $\hat{t} > 0$ and let t^* be such that

$$\sup_{[0,\hat{t}]} \|\nabla e\|^2_{\mathrm{L}_2(\Omega)} = \|\nabla e(t^*)\|_{\mathrm{L}_2(\Omega)} , \tag{A.22}$$

and we replace t, once by t^* and once by $\hat{t}$, we obtain

$$\begin{aligned}\int_0^{t^*} \|\partial_t e\|^2_{\mathrm{L}_2(\Omega)} + \frac{1}{2} \sup_{[0,\hat{t}]} \|\nabla e\|^2_{\mathrm{L}_2(\Omega)} \\ \leq \mathscr{E}(0)^2 + 2\mu \sup_{[0,\hat{t}]} \|\nabla e\|^2_{\mathrm{L}_2(\Omega)} + \frac{1}{4\mu} \left(\mathscr{E}_0(t^*)^2 + \mathscr{E}_1(t^*)^2\right)\end{aligned} \tag{A.23}$$

$$\begin{aligned}\int_0^{\hat{t}} \|\partial_t e\|^2_{\mathrm{L}_2(\Omega)} + \frac{1}{2} \left\|\nabla e(\hat{t})\right\|^2_{\mathrm{L}_2(\Omega)} \\ \leq \mathscr{E}(0)^2 + 2\mu \sup_{[0,\hat{t}]} \|\nabla e\|^2_{\mathrm{L}_2(\Omega)} + \frac{1}{4\mu} \left(\mathscr{E}_0(\hat{t})^2 + \mathscr{E}_1(\hat{t})^2\right)\end{aligned} \tag{A.24}$$

where the $\mathscr{E}$ are defined as

$$\mathscr{E}(0)^2 = \|\nabla e(0)\|^2 + \frac{1}{2}\left(C \|hr(0)\|^2_{\mathrm{L}_2(\Omega)} + C' \left\|h^{1/2} j(0)\right\|^2_{\mathrm{L}_2(\Sigma_h)}\right)$$

$$\mathscr{E}_0(t)^2 := \sup_{[0,t]} \left(C \|hr(t)\|^2_{\mathrm{L}_2(\Omega)} + C' \left\|h^{1/2} j(t)\right\|^2_{\mathrm{L}_2(\Sigma_h)}\right)$$

$$\mathscr{E}_1(t) := \int_0^t C \|h\partial_t r\|_{\mathrm{L}_2(\Omega)} + C' \left\|h^{1/2}\partial_t j\right\|_{\mathrm{L}_2(\Omega)}.$$

(Notice the L_1 nature in time of the last integral above.) By fixing the parameter $\mu = 1/8$ in (A.23) we obtain

$$\frac{1}{4} \|\nabla e(t^*)\|^2_{\mathrm{L}_2(\Omega)} \leq \mathscr{E}(0)^2 + 2\left(\mathscr{E}_0(t^*) + \mathscr{E}_1(t^*)^2\right). \tag{A.25}$$

Inserting this in the right-hand side of (A.24) we obtain

A.3.1 Theorem (Higher order norm estimates for the heat equation)**.** *Let u and u_h be respectively the exact and semidiscrete finite element solution of the Cauchy-Dirichlet problem associated with the heat equation. Then the following aposteriori error estimates holds*

$$\int_0^t \|\partial_t e\|^2_{\mathrm{L}_2(\Omega)} + \frac{1}{4} \|\nabla e\|^2_{\mathrm{L}_2(\Omega)} \leq 2\mathscr{E}(0)^2 + 4\left(\mathscr{E}_0(t)^2 + \mathscr{E}_1(t)^2\right), \tag{A.26}$$

for all $t \in [0,T]$, and

$$\sup_{[0,T]} \|\nabla e\|^2_{\mathrm{L}_2(\Omega)} \leq \mathscr{E}_(0)^2 + 2\left(\mathscr{E}_0(T)^2 + \mathscr{E}_1(T)^2\right). \tag{A.27}$$

Bibliography

[Amb97] Luigi Ambrosio, *Lecture notes on geometric evolution problems, distance function and viscosity solutions*, Pubblicazioni 1029, Istituto di Analisi Numerica del CNR, Pavia, Italy, 1997.

[AO00] Mark Ainsworth and J. Tinsley Oden, *A posteriori error estimation in finite element analysis*, Wiley-Interscience [John Wiley & Sons], New York, 2000. MR 1 885 308

[Bän01] Eberhard Bänsch, *Finite element discretization of the Navier-Stokes equations with a free capillary surface*, Numer. Math. **88** (2001), no. 2, 203–235. MR 1 826 211

[BR78] Ivo Babuška and Werner C. Rheinboldt, *Error estimates for adaptive finite element computations*, SIAM J. Numer. Anal. **15** (1978), no. 4, 736–754. MR 58 #3400

[Bra78] Kenneth A. Brakke, *The motion of a surface by its mean curvature*, Princeton University Press, Princeton, N.J., 1978. MR 82c:49035

[CGG91] Yun Gang Chen, Yoshikazu Giga, and Shun'ichi Goto, *Uniqueness and existence of viscosity solutions of generalized mean curvature flow equations*, J. Differential Geom. **33** (1991), no. 3, 749–786. MR 93a:35093

[Cia78] Philippe G. Ciarlet, *The finite element method for elliptic problems*, North-Holland Publishing Co., Amsterdam, 1978, Studies in Mathematics and its Applications, Vol. 4. MR 58 #25001

[Clé75] Philippe Clément, *Approximation by finite element functions using local regularization*, RAIRO, Rouge, Anal. Numér. **9** (1975), no. R-2, 77–84. MR 53 #4569

[DD00] Klaus Deckelnick and Gerhard Dziuk, *Error estimates for a semi-implicit fully discrete finite element scheme for the mean curvature flow of graphs*, Interfaces Free Bound. **2** (2000), no. 4, 341–359. MR 1 789 171

[Dzi99] Gerhard Dziuk, *Numerical schemes for the mean curvature flow of graphs*, Variations of Domain and Free-Boundary Problems in Solid Mechanics (Paris, 1997), Kluwer Acad. Publ., Dordrecht, 1999, pp. 63–70. MR 2000a:65101

[EG92] Lawrence C. Evans and Ronald F. Gariepy, *Measure theory and fine properties of functions*, CRC Press, Boca Raton, FL, 1992. MR 93f:28001

[EJ91] Kenneth Eriksson and Claes Johnson, *Adaptive finite element methods for parabolic problems. I. A linear model problem*, SIAM J. Numer. Anal. **28** (1991), no. 1, 43–77. MR 91m:65274

[ES91] Lawrence C. Evans and Joel Spruck, *Motion of level sets by mean curvature. I*, J. Differential Geom. **33** (1991), no. 3, 635–681. MR 92h:35097

[FV01] Michael Fried and Andreas Veeser, *Simulation and numerical analysis of dendritic growth*, Ergodic Theory, Analysis, and Efficient Simulation of Dynamical Systems, Springer, Berlin, 2001, pp. 225–252, 812–813. MR 1 850 308

[FV02] Francesca Fierro and Andreas Veeser, *On the a posteriori error analysis for equations of prescribed mean curvature*, Math. Comp. (2002), To appear.

[Giu84] Enrico Giusti, *Minimal surfaces and functions of bounded variation*, Birkhäuser Verlag, Basel, 1984. MR 87a:58041

[GT83] David Gilbarg and Neil S. Trudinger, *Elliptic partial differential equations of second order*, second ed., Springer-Verlag, Berlin, 1983. MR 86c:35035

[HI97] Gerhard Huisken and Tom Ilmanen, *The Riemannian Penrose inequality*, Internat. Math. Res. Notices (1997), no. 20, 1045–1058. MR 98m:53055

[Hui84] Gerhard Huisken, *Flow by mean curvature of convex surfaces into spheres*, J. Differential Geom. **20** (1984), no. 1, 237–266. MR 86j:53097

[Lie96] Gary M. Lieberman, *Second order parabolic differential equations*, World Scientific Publishing Co. Inc., River Edge, NJ, 1996. MR 98k:35003

[MS95] Jean-Michel Morel and Sergio Solimini, *Variational methods in image segmentation*, Birkhäuser Boston Inc., Boston, MA, 1995, With seven image processing experiments. MR 96b:68184

[Neč67] Jindřich Nečas, *Les méthodes directes en théorie des équations elliptiques*, Masson et Cie, Éditeurs, Paris, 1967. MR 37 #3168

[NSV00a] Ricardo H. Nochetto, Giuseppe Savaré, and Claudio Verdi, *A posteriori error estimates for variable time-step discretizations of nonlinear evolution equations*, Comm. Pure Appl. Math. **53** (2000), no. 5, 525–589. MR 2000k:65142

[NSV00b] Ricardo H. Nochetto, Alfred Schmidt, and Claudio Verdi, *A posteriori error estimation and adaptivity for degenerate parabolic problems*, Math. Comp. **69** (2000), no. 229, 1–24. MR 2000i:65136

[SO89] James Sethian and Stanley J. Osher, *The design of algorithms for hypersurfaces moving with curvature-dependent speed*, Nonlinear hyperbolic equations—theory, computation methods, and applications (Aachen, 1988), Vieweg, Braunschweig, 1989, pp. 544–551. MR 991 393

[Son93] Halil Mete Soner, *Motion of a set by the curvature of its boundary*, J. Differential Equations **101** (1993), no. 2, 313–372. MR 94b:58038

[SS00] Alfred Schmidt and Kunibert G. Siebert, *ALBERT—software for scientific computations and applications*, Acta Math. Univ. Comenian. (N.S.) **70** (2000), no. 1, 105–122. MR 1 865 363

[SZ90] L. Ridgway Scott and Shangyou Zhang, *Finite element interpolation of nonsmooth functions satisfying boundary conditions*, Math. Comp. **54** (1990), no. 190, 483–493. MR 90j:65021

[Ura94] Nina N. Uraltseva, *Boundary regularity for flows of nonparametric surfaces driven by mean curvature*, Motion by Mean Curvature and Related Topics (Trento, 1992) (Giuseppe Buttazzo and Augusto Visintin, eds.), de Gruyter, Berlin, 1994, pp. 198–209. MR 96f:53016

[Ver98] Rüdiger Verfürth, *A posteriori error estimates for nonlinear problems: $L^r(0,T;W^{1,\rho}(\omega))$-error estimates for finite element discretizations of parabolic equations*, Numer. Methods Partial Differential Equations **14** (1998), no. 4, 487–518. MR 99g:65099